SYNTHESIS OF Fe_3O_4 AND SILICA COATED Fe_3O_4 NANOPARTICLES BY MICROEMULSION METHOD AND EVALUATION OF ANTIMICROBIAL ACTIVITY

BY

GOSHU ASAB

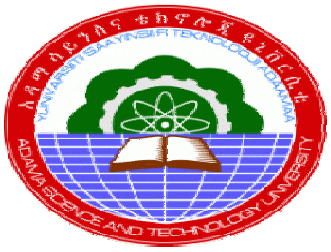

A THESIS SUBMITTED TO THE DEPARTMENT OF CHEMISTRY

SCHOOL OF APPLIED NATURAL SCIENCE

PRESENTED IN PARTIAL FULFILMENT OF THE REQUIREMENT FOR THE DEGREE OF MASTER OF SCIENCE IN CHEMISTRY

OFFICE OF GRADUATE STUDIES

ADAMA SCIENCE AND TECHNOLOGY UNIVERSITY

ADAMA, ETHIOPIA

SEPTEMBER, 2018

SYNTHESIS OF Fe_3O_4 AND SILICA COATED Fe_3O_4 NANOPARTICLES BY MICROEMULSION METHOD AND EVALUATION OF ANTIMICROBIAL ACTIVITY

BY

GOSHU ASAB

ADVISOR: ENYEW AMARE (PhD)

Co-ADVISOR: TESHOME ABDO (PhD)

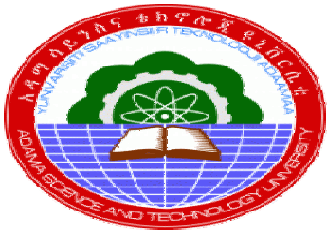

A THESIS SUBMITTED TO THE DEPARTMENT OF CHEMISTRY

SCHOOL OF APPLIED NATURAL SCIENCE

PRESENTED IN PARTIAL FULFILMENT OF THE REQUIREMENT FOR THE DEGREE OF MASTER OF SCIENCE IN CHEMISTRY

OFFICE OF GRADUATE STUDIES

ADAMA SCIENCE AND TECHNOLOGY UNIVERSITY

ADAMA, ETHIOPIA

SEPTEMBER, 2018

APPROVAL OF BOARD OF EXAMINERS

We, the undersigned, members of the Board of Examiners of the final open defense by Goshu Asab have read and evaluated his thesis entitled "**SYNTHESIS OF Fe_3O_4 AND SILICA COATED Fe_3O_4 NANOPARTICLES BY MICROEMULSION METHOD AND EVAIUATION OF ANTIMICROBIAL ACTIVITY**" and examined the candidate. This is, therefore, to certify that the thesis has been accepted in partial fulfillment of the requirement of the Degree of Master of Science in Chemistry.

_____	_____	_____
Advisor	Signature	Date
_____	_____	_____
Co - Advisor	Signature	Date
_____	_____	_____
Chairperson	Signature	Date
_____	_____	_____
Internal Examiner	Signature	Date
_____	_____	_____
External Examiner	Signature	Date
_____	_____	_____
Department Head	Signature	Date
_____	_____	_____
Dean of School of Applied Natural Science	Signature	Date

DECLARATION

I hereby declare that this M.Sc Thesis is my original work and has not been presented for a degree in any other university, and all sources of material used for this thesis have been duly acknowledged.

Name: Goshu Asab

Signature:_____

This M.Sc Thesis has been submitted for examination with our approval as thesis advisors.

Advisor Name: Dr. Enyew Amare (PhD) Co-advisor Name: Dr.Theshome Abdo (PhD)

Signature: _____ Signature: _____

ADVISOR'S APPROVAL SHEET

To: Chemistry Department

Subject: Thesis Submission

This is to certify that the thesis entitled **"SYNTHESIS OF Fe_3O_4 AND SILICA COATED Fe_3O_4 NANOPARTICLESBY MICROEMULSION METHOD AND EVALUATION OF ANTIMICROBIAL ACTIVITY"**submitted in partial fulfillment of the requirements for the degree of Master of Science in Chemistry, the Graduate Program of the Department of Chemistry, and has been carried out by Goshu Asab Id. No GSU/0496/06, under our supervision. Therefore, we recommend that the student has fulfilled the requirements and hence hereby he can submit the thesis to the department.

_____ _____ _____

Name of Advisor Signature Date

_____ _____ _____

Name of Co-Advisor Signature Date

Date of submission:_____

DEDICATION

This Thesis manuscript is dedicated to my mother **Birhane Bezabeh,** for nursing me with affection and love and also dedicated to my beloved wife **Adisalem Zerihun** for her concern, love, patience and affection.

ACKNOWLEDGEMENTS

First I wouldliketothank almightyGodwho gave me strength and wisdom to complete my work successfully.

Then I would like to express my genuine heartfelt gratitude to my advisor, Dr. Enyew Amareforhisinvaluablesuggestion, comments, corrections, professional & technical guidance andfriendlyapproachthroughoutmy work for the successful accomplishment of this thesis.

I would like to express my deepest gratitude to my Co-advisor Dr.Theshome Abdo for his patience, fruitful advice and friendly approach throughout my work.

I would like thank also Kokebe Tsibah secondary and preparatory chemistry teachers who cover my class to do my laboratory work freely.

I would like to express my thanks to the Department of Applied Chemistry, Adama Science and Technology University, for providing me with the necessary knowledge, assistance and facilities to conduct my research work.

I would like to take this opportunity to thank Adama science and Technology University, Department of Material science for allowing me to use TGA and XRD spectroscopy.

I would like to extend my thanks to Addis Ababa University, Department of Chemistry for allowing me to use FT-IR spectroscopy. My thanks also go to Dr. Ananda for assisting me for SEM analysis.

I would like to mention the generous contribution of ASTU biology laboratory academic and research assistant Mr. Urgesafor his cooperation to perform the antimicrobial activity.

My acknowledgement is also extended to Ministry of Education for giving me the opportunity to join this postgraduate program and for sponsorship of my study.

Finally, my cheerful thanks go to my parents and all the family members who give me moral and material support during my study.

TABLE OF CONTENTS

LIST OF TABLES

Tables Page

LIST OF FIGURES

Figures Page

LISIT OF ABBREVATIONS

B.subtilis	Bacillus subtilis
CB	Conduction Band
CTAB	cetyltri methyl ammonium bromide
D	Crystallite size
DLS	dynamic light scattering
E. coli	Escherichia coli
EU	European union
FTIR	Fourier Transforms Infrared
HLB	hydrophil lipophile balance
MNps	Magnetite Nanoparticle
Nm	Nano meter
NM	Nanomaterial
NNI	National Nano Technology Initiative
Nps	Nanoparticles
NSM	Nanostructure Material
O/w	Oil in Water
Ps.aeruginosa	Pseudomonas aeroginosa
ROS	Reactive Oxygen Species
S.aureus	Staphylococcus aureus
SDS	Sodium Dodecyl Sulfate
SEM	Scanning Electro microscop
TEOS	Tetraethyl orthosilicate
VB	Valance Band
W/O	Water in oil
WHO	World health organization
XRD	X-ray diffraction

ABSTRACT

The Present work outlines the antimicrobial activity of Fe_3O_4 nanoparticles synthesized through micro emulsion method from hydrated ferric nitrate and ferrous sulfate as precursor material and ammonia as precipating agent with the assistant of Tween -80 and SDS surfactants. The obtained Fe_3O_4 nanoparticles were characterized by X-ray diffraction, Scanning electron microscopy, Thermogravimetry-Differential thermal analyzer and Infrared Spectroscopy. X-ray diffraction and Fourier transforms Infrared spectra showed that the Fe_3O_4 NPs was phase pure with cubic inverse spinel structure & presence of Fe-O bond respectively. The crystallite size determined from XRD using Scherrer's equation was in the range of 7.5-10.83 nm for uncoated Fe_3O_4 and 16 nm for silica coated Fe_3O_4 Nps. SEM results showed that the bare Fe_3O_4 nanoparticles morphologies heterogeneous and agglomerated. But the silica coated Fe_3O_4 Nps was relatively homogeneous without any substantial agglomeration. The Fe_3O_4 Nps size slightly increases with the temperature and precursor concentration. The antimicrobial activity of Fe_3O_4 nanoparticles tested against Gram-negative (Escherichia coli and *Pseudomonas aeruginosa) and Gram-positive (Staphylococcus aureus* and *Bacillus subtilis) bacteria exhibited good antimicrobial activity.*

Keywords

Magnetite nanoparticles, microemulsion, characterization, antimicrobial activity

1. INTRODUCTION

1.1. Background of the Study

In the last two decades, nanotechnology has attracted great interest in several areas of research for the development of nanoscaled material. Nanotechnology abbreviated to "**Nanotech**", is the study of manipulating matter on an atomic and molecular scale (Sun deep et al., 2010). Generally nanotechnology deals with structures sized between 1 to 100 nm and involve developing materials or devices within that size. Nanotechnology has the capacity to improve our ability to prevent, detect, and remove environmental contaminants in air, water, and soil in a cost effective and environmental friendly manner (Arivalagan K. et al., 2011).

Nanoparticles are typically defined as tiny solids, whose dimensions do not exceed 100 nm in all the three directions (Willard et al, 2004). Due to their size (diameters ranging from 1 to 100 nm) nanoparticles present specific and controllable properties that are different from those they present on the macroscopic scale thus enabling unique applications (Srivastava et al, 2009). The change in properties is due to two main effects: Surface effects or size reduction effect (when particle size is reduced, a greater proportion of atoms are found at the surface) and Quantum confinement-modification in electronic structure.

Iron oxide is a mineral compound which occurs abundantly in nature. It presents more than one crystal structure and also different structural and magnetic properties. The main forms of these minerals are hematite, magnetite and maghemite. Crystal structure of the three oxides can be defined in terms of close packed planes of oxygen anions with iron cations in octahedral or tetrahedral interstitial sites (Baby et al. 2015). Among all iron oxides, magnetite Fe_3O_4 possess the most interesting properties because of the presence of iron cations in two valence states, Fe^{3+} and Fe^{2+} in the inverse spinel structure. The cubic spinel Fe_3O_4 is ferrimagnetic at temperatures below 858 K (Gubin Y. A. et al, 2005).

Magnetic iron oxide nanoparticles have a large surface-to-volume ratio so hold high surface energies. Therefore, they are disposed to aggregate for the purpose of minimize the surface energies. Furthermore, the naked iron oxide nanoparticles have high chemical activity, and they are also easily oxidized in air (especially magnetite), so that they lose of magnetism and

dispersibility. For this reason, appropriate surface coating to protect the stability of magnetic iron oxide nanoparticles is very important (Wu W. et al, 2008).

In recent years, nanoscale transition of metallic oxides, such as iron oxide, including hematite, magnetite, and maghemite, has been attracting growing interest as they exhibit unique electrical, optical and magnetic properties for numerous applications such as production of inorganic pigments, magnetic storage media, development of gas sensors as well as electronic and optical devices, information storage, color imaging, magneto caloric refrigeration, bioprocessing, ferrofluid technology and wastewater treatment adsorbents (Moahapatra et al , 2010).

Recently, numerous researches have been, focused on novel synthetic methodologies for well-controlled nanomaterial, including controlled size and shape, which are important for their chemical and physical properties. A wide range of techniques has been, developed for the preparation of nanomaterials. These techniques include physical methods such as mechanical milling (Arbain et al. 2011) and inert gas condensation. Along with chemical methods such as chemical reduction, photochemical reduction, electro deposition, hydrothermal, sol-gel and micro emulsion synthesis are some of them (Mohanty et al, 2011).

Among all chemical methods, the micro emulsion method has been, demonstrated as a very versatile and reproducible technique that allows to control over the nanoparticle size and yield nanoparticles at low temperature with a narrow size distribution (Lopez-Quintela et al, 2003). Micro emulsion is a thermodynamically stable dispersion of two immiscible fluids facilitated by surfactant molecules. A micro emulsion has ultralow interfacial tension, large interfacial area and capacity to solubilize both aqueous and oil soluble compounds. The synthesized particle size depends on the water content in micro emulsion system. The increase of particles size is obtained with increasing the water fraction in water in oil (W/O)micro emulsion (Wongwailikhit and Horwongsakul, 2011). The advantage of the method is the ability to control the particle size and morphology easily by adjusting the concerned parameters.

Many transition metal oxides nanoparticles including ZnO, TiO_2, CuO, Fe_2O_3 and Fe_3O_4 were studied for antibacterial activity. The reason for the bactericidal activity is due to the presence of reactive oxygen species (ROS) generated by different metal oxides nanoparticles (Prabhu Y.T et

al, 2015). Antibacterial activity is related to compounds that locally kill bacteria or slow down their growth, without being in general toxic to surrounding tissue. According to their structure, components, and functions, the bacteria cell wall can be divided into the two main categories: Gram positive (+) and Gram negative (–). Resistance to currently used antibiotics is a serious public health problem nowadays. Novel antibiotics are needed to effectively treat infections caused by these resistant strains. The nanoparticles have been extensively evaluated for their potential as suitable antibacterial candidates which may be developed as antibacterial therapy for clinical application (Shakeel Ahmed Ansari, 2017).

Due to their excellent properties, magnetite nanoparticles (MNPs) have proved a great potential for diverse applications in nanobiotechnology, such as drug targeting and delivering , magnetic resonance imaging, inhibition of microbial biofilm development (Saviuc et al ,2011), optimization of wound dressings , stabilization of essential oils and antitumor therapy.

Therefore, the aims of this study are to synthesis Fe_3O_4 nanoparticles by micro emulsion methods and assess its antimicrobial activity.

1.2. Statement of the Problem

Antibiotics have been a mainstay of human health and extensively used in clinics to treat respiratorytract infections, urinary tract infections, gastrointestinalinfections and infections of nervous system (Singh, R. et al, 2014). However, the emergence of multidrug resistant bacterial strains suchas Methicillin resistant *staphylococcus aureus* (MRSA), Vancomycin resistant *staphylococcus aurous* (VRSA), has severely compromised their effectiveness in the clinics. Therefore, novel antibiotics with newer mechanism of action are urgently needed to treat infections caused by MDR-bacterial strains. Fe_3O_4-NPs-basedbiomedical applications have received considerable attention due to their ease of laboratory synthesis; cost effectiveness, physical and chemical stability, as well as biocompatibility and environmental safety. Therefore, Fe_3O_4-NPs may be reasonable candidates for their potentialuse as antibacterial therapy.

Synthesis of controllable size nanoparticles for different application is difficult. There are various synthesis methods for nanoparticles including precipitation, hydrothermal; sol-gel and microemulsion. Precipitation synthesis involves dissolution of compound salt precursor in

aqueous media and subsequent precipitation from the solution by pH adjustment. The precipitation technique is probably the simplest and most efficient chemical pathway to obtain metal oxide nanoparticles. However, the control of particle size distribution is limited, because only kinetic factors are controlling the growth of the crystal. In hydrothermal synthesis, metal salts dissolved in aqueous media in a sealed container and heated above the boiling temperature of water, and consequently the reaction pressure is increased much above atmospheric pressure. Unfortunately, there is no straight forward way to control the size and the shape of the final particles as compare to the micro emulsion technique. Sol-gel method is based on the hydroxylation and condensation of molecular precursors in solution, (Srivastava et al, 2009) originating a "sol" of nanometric particles. But it is thermodynamically unfavorable and form large agglomeration. A micro emulsion is a transparent and thermodynamically stable solution of low viscosity that forms spontaneously from the mixture of surfactant, water and oil. Microemulsion-based synthesis is a powerful method whereexpensive or specialized instruments are not needed, contrastingto the case for several physical methods such as plasmasynthesis, ball milling and chemical vapor deposition. In addition it synthesized at low temperature, no need of calcinations and allows particle size to be controlled just by controlling the droplet size. These are the advantage of microemulsion over other methods. Therefore, in this work Fe_3O_4 Nps and silica coated Fe_3O_4 Nps were synthesized by micro emulsion method using the surfactant of Tween-80 and SDS to get controllable size nanoparticles for biomedical application.

1.3. Objective of the Study

1.3.1. General Objective

Synthesis and characterization of Fe_3O_4 and silica coated Fe_3O_4 nanoparticles prepared by micro emulsion method and evaluation of antimicrobial activity.

1.3.2. Specific Objectives

The specific objectives of this work are:

- To Synthesize Fe_3O_4 and silica coated Fe_3O_4 nanoparticles by micro emulsion method using Tween-80 and SDS.
- To characterize Fe_3O_4 and silica coated Fe_3O_4 nano particles synthesized with Tween-80 and SDS using XRD, SEM, TGA and FTIR spectroscopy.
- To study the influence of surfactants, temperature and precursor concentration on the particle size.
- To investigate antimicrobial activity of Fe_3O_4 and silica coated Fe_3O_4 nanoparticles against Gram-negative and Gram-positive bacteria and Candida ablicans fungi.

1.4. Significance of the Study

This study provides important information about the synthesis strategy of Fe_3O_4 and silica coated Fe_3O_4 nanoparticles and its antibacterial and antifungal investigation.

1.5. Scope of the Study

This work is limited to the synthesis of Fe_3O_4 nanoparticles via microemulsion method using Tween-80 and SDS as a surfactant, and silica coated Fe_3O_4 nanoparticle using Tween -80 at 30^oC. The characterization also limited FT-IR, XRD, TGA and SEM. In addition, the antimicrobial test also limited Gram-negative (*Escherichia coli* and *Pseudomonas aeruginosa*) and Gram-positive (*Staphylococcus aureus* and *Bacillus subtilis*) bacteria and Candida ablicans fungi.

2. LITRATURE REVIEW

2.1. Nanotechnology

In the past few decades, a word "nano" attracted enormous attention, interest and investigation around the world. "Nano" means one billionth (10^{-9}), so 1 nanometer refers to 10^{-9} meter and is expressed as 1 nm. One nm is so small that things smaller than it can only be molecules, clusters of atoms or particles in the quantum world. Nanotechnology is a rapidly growing research field with an increasing impact on our everyday lives. The field of nanotechnology can be defined as the production and use of materials at the nanoscale, normally characterized as smaller than 100 nm in one dimension (Oberdorster et al, 2007).

Nowadays nanotechnology is very important for the advancement of science, since it makes use of the manipulation of matter on a scale in which materials show different characteristics than those displayed in the micro and macro scale. There are no exact definitions for nanoscience and nanotechnology. The following is the definition of nanoscience and nanotechnology given by the U.S. National Nanotechnology Initiative (NNI): nanoscience and nanotechnology are "Research and technology development at the atomic, molecular and macromolecular levels in the length scale of approximately the 1-100 nanometer range, to provide a fundamental understanding of phenomena and materials at the nanoscale and to create and use structures, devices and systems that have novel properties and functions because of their small and/or intermediate size"(Soler-Illia,2002). Nanoscience and nanotechnologies are revolutionizing our understanding of matter and are likely to have profound implications for all sectors of the economy, including agriculture and food, energy production and efficiency, the automotive industry, cosmetics, medical appliances and drugs, household appliances, computers, and weapons (Arivalagan K. et al, 2011). Nanotechnology has the capacity to improve our ability to prevent, detect, and remove environmental contaminants in air, water, and soil in a cost effective and environmentally friendly manner (Arivalagan K. et al, 2011).

2.1.1. Nanomaterial

According to EU in 2011 , nanomaterials define as "a natural, incidental or manufactured material containing particles, in an unbound state or as an aggregate or as an agglomerate and where, for 50% or more of the particles in the number size distribution, one or more external

dimensions is in the size range 1 nm-100nm"(EU, 2011). On the basis of particle size the nanomaterials are classified into following major types *viz:* Nanoparticles, Nanocapsules ,Fullerenes, Dendrimers, Quantum dots, Nanostructures, Nanopores.

2.1.2. Nanoparticles

Nanoparticles are the building blocks of nanotechnology. Nanoparticles are particles which are 1 to 100 nanometers in size. In nanotechnology, a particle is defined as a small object that behaves as a whole unit with respect to its transport and properties. The particles are further classified according to diameter; ultrafine particles are the same as nanoparticles and between1 and 100 nanometers in size. Coarse particles cover a range between 2,500 and10,000 nanometers. Fine particles are sized between 100 and 2,500 nanometers.

Nanoparticles are generally classified based on their dimensionality, morphology, composition, uniformity, and agglomeration. Nanoparticles can be classified on the basis of dimensions as zero; one, two and three dimensions (Pokropivny et al, 2007).

2.1.2.1. Zero Dimension Nanoparticles (0DNps)

The most common representation of zero-dimensional nanomaterials are nanoparticles. Recently, 0D NSMs such as uniform particles arrays (quantum dots), heterogeneous particles arrays, core–shell quantum dots, onions, hollow spheres and nanolenses have been synthesized by several research groups (Jitendra. et al, 2012). Moreover, 0D NSMs, such as quantum dots has been extensively studied in light emitting diodes (LEDs), solar cells, single-electron transistors, and lasers.

Quantum Dots (QDs):

Quantum dots are small particles that contain a tiny droplet of free electrons. QDs are colloidal semiconductor nanocrystals ranging from 2 to 10 nm in diameter. QDs can be synthesized from various types of semiconductor materials via colloidal synthesis or electrochemistry. The most commonly used QDs are cadmium selenide (CdSe), cadmium telluride (CdTe), indium phosphide (InP), and indium arsenide (InAs).Quantum dots can have anything from a single electron to a collection of several thousands. QDs have been developed in a form of semiconductors, insulators, metals, magnetic materials or metallic oxides. It can be used for

optical and optoelectronic devices, quantum computing, and information storage. Colour coded quantum dots are used for fast DNA Testing.

2.1.2.2. One Dimension Nanoparticles (1D NP's)

Materials with one dimension in the nanometer scale are typically thin films or surface coating. One dimensional system, such as thin film or manufactured surfaces, has been used for decades in electronics, chemistry and engineering. Production of thin films (sized 1-100 nm) or monolayer is now common place in the field of solar cells or catalysis. These thin films are using in different technological applications, including information storage systems, chemical and biological sensors, and fiber-optic systems, magneto-optic and optical device. 1D Nps are needle like-shaped nanomaterials. 1-D materials include nano rods and nano wires.

2.1.2.3. Two Dimension Nanoparticles

Two-dimensional nanomaterials have two dimensions in the nanometer scale. 2-D nanomaterials exhibit plate-like shapes. Two-dimensional nanomaterials include nanofilms, nanolayer, nanotubes and nanocoatings. Carbon nanotubes are hexagonal network of carbon atoms, 1 nm in diameter and 100 nm in length, as a layer of graphite rolled up into cylinder. CNTs are of two types, single walled carbon nanotubes (SWCNTs) and multi-walled carbon nanotubes (MWCNTs). The small dimensions of carbon nanotubes, combined with their remarkable physical, mechanical and electrical properties, make them unique materials. They display metallic or semi conductive properties, depending on how the carbon leaf is wound on itself.

2.1.2.4. Three Dimension Nanoparticles

Materials that are nanoscaled in all three dimensions are considered 3D nanomaterials. These include:

Fullerenes (Carbon 60):

Fullerenes are spherical cages containing from 28 to more than 100 carbon atoms. This is a hollow ball composed of interconnected carbon pentagons and hexagons, resembling a soccer ball. Fullerenes are class of materials displaying unique physical properties. They can be subjected to extreme pressure and regain their original shape when the pressure is released.

Dendrimers:

Dendrimers represent a new class of controlled-structure polymers with nanometric dimensions. They are considered to be basic elements for large-scale synthesis of organic and inorganic nanostructures with dimensions of 1 to 100 nm.

2.2. Methods of Synthesizing Nanoparticles

There are three basic methods for the synthesis of nanoparticles named as physical method, Chemical method and biological method (Luechinger et al, 2010). In the top-down (physical) approach onestarts from a bulk material and attempts to break it down into nanoscale objects through physical methods. Bottom-up (chemical) approach refers to the buildup of a structure from the bottom, i.e., atom-by-atom, molecule-by-molecule, or cluster-by cluster, growing from a solution. This technique has been attractive for researchers, primarily because of the simplicity with which experiments can be conducted in the laboratory. Scaling the process to production of industrial-scale quantities of powders is, however, not as straight forward. The further classifications of the synthesis methods of nanoparticles as given in table 1.

Table 1: Classification of methods of synthesizing nanoparticle

Physical method	Biological method	Chemical method
Arc discharge method	By plant extraction	Co-precipitation
Electron beam method	By micro organism	Sono-chemical
Lithography	By algae	Electrolysis
Ion implantation	By biomolocule or enzyme	Micro emulsion
Inert gas condensation	By agriculture & industry	Chemical reduction
Mechanical grinding	-------	Phytochemical
Milling	--------	Solo-gel
Spary pyrolysis	---------	Pyrolysis
Vapour phase synthesis	---------	Solvothermal

Approaches for the Synthesis of Nanoparticles, (Rani et al, 2014)

The details of various chemical methods for nanoparticles preparation including:

2.2.1. Precipitation and/or Co-Precipitation method

Co-precipitation synthesis involves dissolution of compound salt precursor in aqueous media and subsequent precipitation from the solution by pH adjustment. The precipitation technique is probably the simplest and most efficient chemical pathway to obtain iron oxide particles. Iron oxides (FeOOH, Fe_3O_4 or Υ-Fe_2O_3) are usually prepared by addition of alkali to iron salt solutions and keeping the suspensions for ageing. The main advantage of the precipitation process is that a large amount of nanoparticles can be synthesized. However, the control of particle size distribution is limited, because only kinetic factors are controlling the growth of the crystal. The co-precipitation method is considered as the simplest chemical way to synthesize iron oxide nanoparticles. Performed first time by Massart more than 30 years ago, it had several modifications, but it`s main chemistry didn`t change.

$$Fe^{2+} + Fe^{3+} + 8OH^- \longrightarrow Fe_3O_4 + 4H_2O$$

The reaction is not direct; a formation of some iron complexes takes place:

$$Fe^{3+}(H_2O)_6 \longrightarrow FeOOH + 3H^+ + 4H_2O$$

$$Fe^{2+} + 2OH^- \longrightarrow Fe(OH)_2$$

$$2FeOOH + Fe(OH)_2 \longrightarrow Fe_3O_4 + 2H_2O$$

Fe^{2+} and Fe^{3+}ions in molar ratio of 1:2 precipitate into magnetite in a basic solution (pH from 8 to 14)

2.2.2. Hydrothermal Synthesis

Hydrothermal synthesis is an alternative technique for the preparation of highly crystalline metal oxide NPs (Wang et al., 2005). In hydrothermal synthesis, metal salts dissolved in aqueous media in a sealed container and heated above the boiling temperature of water, and consequently the reaction pressure is increased much above atmospheric pressure. The high temperatures and pressures strongly improve the quality of the nano crystals and their magnetic features. Unfortunately, there is no straightforward way to control the size and the shape of the final particles as compare to the micro emulsion technique.

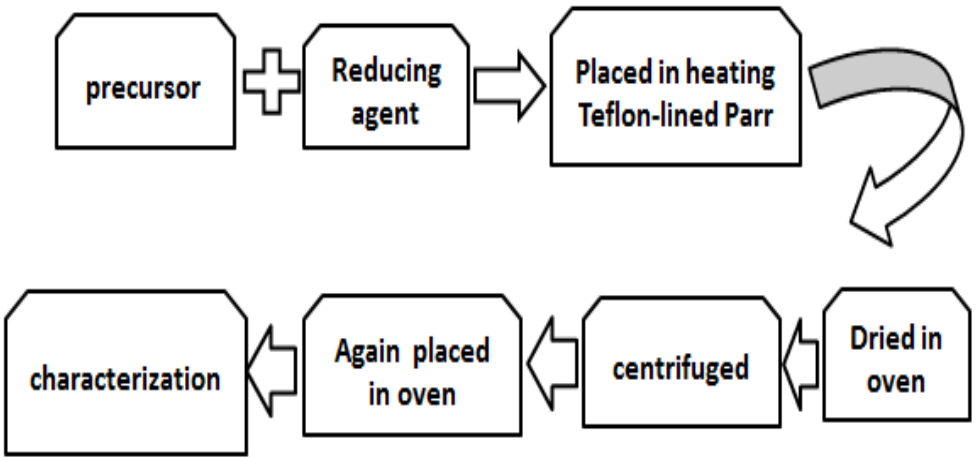

Figure 1: Schematic of synthesis of nano particles by hydrothermal method

2.2.3. Sol-Gel Method

The sol-gel process is a suitable wet route to the synthesis of nanostructure metal oxides. This method is based on the hydroxylation and condensation of molecular precursors in solution, (Srivastava et al, 2009) originating a "sol" of nanometric particles. The ''sol'' is then dried or ''gelled'' by solvent removal or by chemical reaction to get three dimensional metal oxide network. Gel properties are very much dependent upon the structure created during the sol stage of the sol-gel process. The solvent used is generally water, but the precursors can also be hydrolyzed by an acid or base. Basic catalysis induces the formation of a colloidal gel, whereas acid catalysis yields a polymeric form of the gel. These reactions are performed at room temperature; further heat treatments are needed to acquire the final crystalline state.

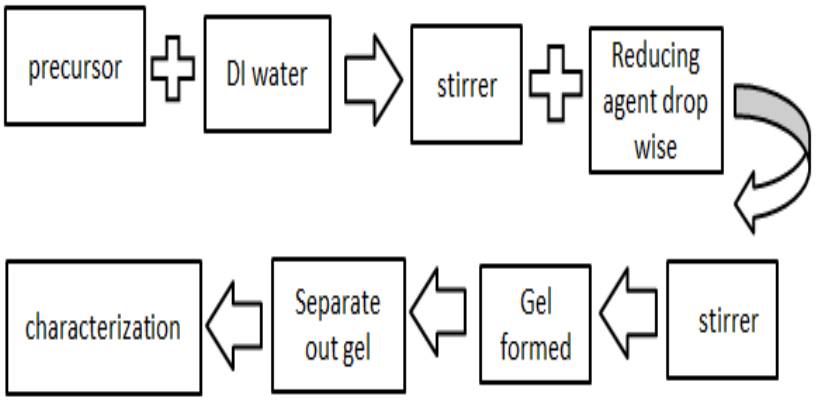

Figure 2: Schematic of synthesis of nanoparticles by sol gel methods

2.2.4. Micro emulsion Method

The concept of micro emulsions was first introduced by Professor, Jack H. Schulman at Columbia University in 1959. Uniformly sized MNPs can be synthesized using water-in-oil (W/O) microemulsion, an isotropic and thermodynamically stable single-phase system, with three components: water, oil and an amphiphilic molecule, called surfactant, which lowers the interfacial tension between water and oil, forming a transparent solution. MNPs are synthesized by mixing, precipitation reaction and aggregation processes resulting from the rapid coalescence of water nanodroplets containing reagents as nanoreactor. The surfactant molecules surround the nanodroplets walls of the spherical water pool, which serve as cages for the growing particles, reducing the average size of the particles during the collision and aggregation process. Mixing two identical water-in-oil microemulsions containing the desired reactants leads to micro droplets continuously colliding, coalescing and breaking, eventually forming a precipitate in the micelles. In reverse microemulsion, aqueous solution disperses in the organic phase, inside the self-assembly reverse micelles, forming several monodisperse nano-droplets. The advantage of the confined nanoreactor environment within the reverse micelle is that it yields highly monodisperse NPs and increases the incorporation of nonbonded non-polar molecules. Depending on the composition three types of microemulsion are most likely to be formed.

1. Oil in water (O/W) micro emulsion where oil droplets are dispersed in a continuous aqueous phase
2. Water in oil (W/O) micro emulsion where water droplets are dispersed in a continuous oil phase
3. Bicontinuous micro emulsion where micro domains of oil and water are interdispersed within the system

Micelles are the simplest structures: spherical orcylindrical objects formed by surfactant molecules, separating oil and water molecules. Micelles are likedrops of oil in water and reverse micelles are like dropsof water in oil (Danielson and Lindeman, 1981). The synthesis of nanoparticles by reverse micro emulsions is viable and attractive because it does not only produce nanoparticles that have a narrow size distribution, but also the particle size can be controlled by varying the micro emulsion composition (Fernandez et al., 2007).

A micro emulsion is a transparent and thermodynamically stable solution of low viscosity that forms spontaneously from the mixture of surfactant, water, and oil. The preparation of magnetic iron oxide nanoparticles with controlled size and morphology has been carried out in water-in-oil micro emulsion consisting of a cationic or non-ionic surfactant (Triton-X), a co-surfactant (glycols, hexanol, and 1-butanol), oil phase (n-octane, cyclohexane) and aqueous phase (Fernandez et al. 2013). Microemulsion-based synthesis is a powerful method where expensive or specialized instruments are not needed, contrasting to the case for several physical methods such as plasma synthesis, ball milling, chemical vapor deposition etc.

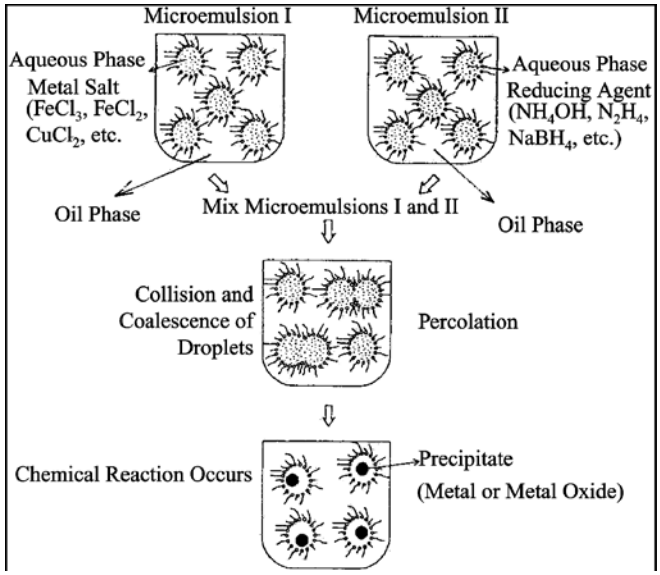

Figure 3: Proposed mechanism for the formation of nanoparticles by the micro emulsion approach

The water-in-oil emulsions are currently being used to synthesize super paramagnetic iron oxide nanoparticles with a narrow size range and uniform physical properties because of the ability to control the size and shape of the nanoparticles. This system is formed by well-defined nanodroplets of the aqueous phase, dispersed by the assembly of surfactant molecules in a continuous hydrocarbon phase. The main advantage of using this type of emulsion system is that the size of the nanoparticles can be controlled by modulating the size of the aqueous droplets core. Indeed, using variable reaction temperatures results in magnetites with diameters of 3-12 nm. The metal and base concentrations can also be used to vary the nanoparticle size (Pileni M. P et al, 2003). Salazar-Alvarez has reported the synthesis of iron oxide nanoparticles by the use

of reverse emulsions. The nanoemulsion system consisted of AOT BuOH/cHex/H_2O, with a surfactant/water molar ratio of 2.85 and a surfactant/ co surfactant molar ratio of 1. A sequential synthetic procedure was used to prepare the nanoparticles. One nanoemulsion containing the iron source and another containing a solution of sodium hydroxide were mixed to form the magnetite nanoparticles. The nanoemulsion was lysed with acetone to remove the particles from the surfactant and washed several times with ethanol. The colloidal nanoparticles exhibit super paramagnetic behavior with high magnetization values.

The oil and water phases often contain several dissolved components, and therefore, the selection of the surfactant (and co surfactant) depends upon the physicochemical characteristics of the system. Several types of surfactants, such as cationic, anionic, or non-ionic, can be used. The literature often reports the use of sodium bis (2-ethylhexylsulfosuccinate) (AOT), cetyltrimethylammonium bromide (CTAB), or sodium dodecylsulfate (SDS) as ionic surfactants. Unfortunately, the ionic surfactants functional group in the hydrated core seems to limit the capability of forming highly crystalline magnetite nanoparticles. The use of non-ionic surfactants, such as polyethoxylates (Triton X-100, Igepal CO-520, Tween-80 and Brij-97), avoids the complication of the presence of a complexing functional species and offers great future potential (Santra S. et al, 2001).

2.2.4.1. Surfactant in Micro emulsion

Surfactants are wetting agents that lower thesurface tension of a liquid, allowing easier spreading, and can also lower the interfacial tension between two liquids. Surfactants are usually organic compounds that are amphipathic, as they contain both hydrophobic groups ("tails") and hydrophilic groups("heads"). Therefore, they are soluble in both organic solvents and water. Surfactants are indicated by the presence of both polar and non polar region. Normally surfactants are classified according to their structure into ionic, zwitterionic and non ionic according to their charges. Tween-80 is an example of non ionic surfactant which is non-toxic, environmental friendly, biocompatible and commercially inexpensive (Cristina Prieto et al, 2013).

Introduction of co-surfactants provides further reduction in the surface tension and fluidizes the interfacial surfactant film which can expand the area of existence of microemulsion system

(Chauhan et al, 2012). Co surfactants are added to obtain nanoemulsion systems at low surfactant concentration. Short to medium-chain-length alcohols (C_3–C_8) are commonly added as co surfactants, which further reduce the interfacial tension and increase the fluidity of the interface. They also increase the mobility of the hydrocarbon tail and allow greater penetration of the oil into this region.

Hydrophile – Lipohile Balance (HLB) was a method proposed by Griffin, as a guide to select an optimal emulsifying agent. In general a lower HLB number is used for water in oil (W/O) emulsifications while a higher HLB number is used for oil in water (O/W) emulsifications. The HLB value of the surfactant indicates the solubility of the surfactant. If the surfactant has lower HLB value then surfactant is more lipophilic or oil soluble or if the surfactant has higher HLB value then surfactant is more hydrophilicor water soluble. Griffin proposed an HLB scale for non-ionic surfactants and the HLB number 1 was assigned to the most lipophilic molecule while 20 was assigned to the most hydrophilic molecule.

2.3. Characterization of Nanoparticles

2.3.1. X-ray Diffraction

Now a day, X-ray diffraction is most extensively used technique for the characterization of the materials. A lot of information can be extracted from the XRD data. Using this technique, one can get the information regarding the crystalline nature of a material, nature of the phase present, lattice parameter and grain size (Liu, D. et al, 1995). From the position and shape of the lines, one can obtain information regarding the unit cell parameters and microstructural parameters (grain size, microstrain, etc), respectively. The interaction of X-ray radiation with crystalline sample is governed by Bragg's law, which depicts a relationship between the diffraction angles (Bragg angle), X-ray wavelength, and interplanar spacing of the crystal planes. According to Bragg's law, the X-ray diffraction can be visualized as X-rays reflecting from a series of crystallographic planes. The path differences introduced between a pair of waves travelled through the neighboring crystallographic planes are determined by the interplanar spacing. If the total path difference is equal to $n\lambda$ (n being an integer), the constructive interference will occur and a group of diffraction peaks can be observed, which give rise to X-ray patterns. The quantitative account of Bragg's law can be expressed as:

$$2d_{hkl}\sin\theta=n\lambda \quad \ldots\ldots 1$$

where d is the interplanar spacing for a given set of *hkl* and θ the Bragg angle. The diffraction method is based on the effect of broadening of diffraction reflections associated with the size of the particles (crystallites). The size of nanomaterials can be derived from the peak broadening and can be calculated by using the Scherrer equation that is given below in equation 2.

$$D = \frac{0.94\lambda}{\beta cos\theta} \quad \ldots\ldots 2$$

Where D is the average crystalline diameter, 0.94 is the Scherer's constant, λ is the X-ray Wavelength, ß is the line broadening at half the maximum intensity and θ is the Bragg's angle in degree.

2.3.2. Scanning Electron Microscopy (SEM)

Electron microscopes are scientific instruments that use a beam of energetic electrons to examine objects on a very fine scale. This electron microscopy based technique determines the size, shape and surface morphology with direct visualization of the nanoparticles. Therefore scanning electron microscopy offer several advantages in morphological and sizing analysis. During the process of SEM characterization, solution of nanoparticles should be initially converted into a dry powder. This dry powder is then further mounted on a sample holder followed by coating with a conductive metal (e.g. gold) using a sputter coater. Whole sample is then analyzed by scanning with a focused fine beam of electrons (Jores k.et al, 2004). Secondary electrons emitted from the sample surface determine the surface characteristics of the sample. This electron beam can often damage the polymer of the nanoparticles which must be able to withstand vacuum. Average mean size evaluated by SEM is comparable with results obtained by dynamic light scattering.

2.3.3. Dynamic Light Scattering (DLS)

Current research demands the fastest and most popular method of determining particle size. The fastest and most popular techniques like photon-correlation spectroscopy (PCS) or dynamic light scattering (DLS), widely used to determine the size of Brownian nanoparticles in colloidal suspensions in the nano and submicron ranges. In this technique solution of spherical particles in

Brownian motion causes a Doppler shift when they are exposed against shining monochromatic light (laser). Such monochromatic light exposure hits the moving particle which results in changing the wavelength of the incoming light. Extent of this change in wavelength determines the size of the particle. This parameter assists in evaluation of the size distribution, particle's motion in the medium, which may further assists in measuring the diffusion coefficient of the particle and using the autocorrelation function. Dynamic light scattering (DLS) offer the most frequently used technique for accurate estimation of the particle size and size distribution (DeAssis DN, et al, 2008).

2.3.4. Infrared Spectroscopy

Infrared (IR) spectroscopy is a popular characterization technique in which a sample is placed in the path of an IR radiation source and its absorption of different IR frequencies is measured (Sisler, H.W., et al, 1980). Solid, liquid, and gaseous samples can all be characterized by this technique. IR photons energies, in a range between 1 to 15 kcal/mol, are insufficient to excite electrons to higher electronic energy states, but transitions in vibrational energy states. These states are associated with a molecule's bonds, and consequently each molecule has its own unique signatures. Therefore, IR spectroscopy may be employed to identify the type of bond between two or more atoms and consequently identify functional groups. IR spectroscopy is also widely used to characterize the attachment of organic ligands to organic/inorganic nanoparticles and surfaces. Because IR spectroscopy is quantitative, the number of a type of bond may be determined. More complex molecules contain dozens or even hundreds of different possible bond stretches and bending motions, which implies the spectrum may contain dozens or hundreds of absorption lines. This means that the IR absorption spectrum can be its unique fingerprint for identification of a molecule.

2.3.5. UV-Visible Spectroscopy

Ultraviolet-visible (UV-vis) spectroscopy is widely utilized to quantitatively characterize organic and inorganic nanosized molecules. A sample is irradiated with electromagnetic waves in the ultraviolet and visible ranges and the absorbed light is analyzed through the resulting sprectrum (Perkampus, H. H, 1992). It can be employed to identify the constituents of a substance, determine their concentrations, and to identify functional groups in molecules. The samples can

be either organic or inorganic, and may exist in gaseous, liquid or solid form. Different sized materials can be characterized, ranging from transition metal ions and small molecular weight organic molecules, whose diameters can be several Ångstroms, to polymers, supramolecular assemblies, nano-particles and bulk materials. Many electronic properties, such as the band gap of a material, can also be determined by this technique.

2.4. Oxides of Iron

Iron oxides are one of the most important transition metal oxides of technological importance. It is found in nature in different forms. Magnetite Fe_3O_4, Maghemite, ɣ-Fe_2O_3, and hematite, α-Fe_2O_3 are the most common among them (Babay et al., 2015). Nanostructure iron oxides are a great interest when compared with their bulk counterpart due to their large surface area, high rate of reactivity, and due to the possibility of enhancing environmentally friendly reactions. They have superior characters in nontoxicity, chemical stability, durability, and are low costs (Legodi *et al*., 2007). Iron oxides are compounds available in nature and easily synthesize in laboratory. Iron oxide NPs are superior to other metal oxide NPs for their biocompatibility and stability and are the most commonly employed magnetic NPs for biomedical applications. From all the iron oxides, Fe_3O_4 (magnetite) has the most interesting magnetic properties due to the presence of iron cations in two valence states, Fe^{2+} and Fe^{3+}.

Crystal structure of the three oxides can be defined in terms of close packed planes of oxygen anions with iron cations in octahedral or tetrahedral interstitial sites. Because of its polymorphism magnetite (Fe_3O_4) is one of the most interesting crystallographic phases of iron oxide, especially in its nanosized forms. It exhibits four different crystalline polymorphs with unique magnetic properties. The main forms, hematite (α-Fe_2O_3) and maghemite (ϒ-Fe_2O_3) occur in nature and the other oxides in the forms beta (β-Fe_2O_3) and epsilon (Є-Fe_2O_3) are nanometric structures whichare generally synthesized in laboratory (Machala et al. 2011).

2.4.1. Hematite (α-Fe_2O_3)

Hematite, α-Fe_2O_3, is the most known of iron oxides and the most frequent polymorph which exists in nature as mineral (Machala et al. 2011), occurring widely in rocks and soils. It is an oxide with a weak ferromagnetic or anti-ferromagnetic behavior at room temperature. Furthermore, above 956 K it is paramagnetic. Hematite is easier to synthesize than the other

forms of oxide as it is the end product of other iron oxide forms of transformation and isalso extremely stable under environmental conditions (Machalaet al. 2011; Cornell and Schwertmann 2000).

Hematite is widely used in catalysts, pigments and gas sensors due to its low cost and high resistance to corrosion. It can also be used as a starting material for the synthesis of magnetite (Fe_3O_4) and maghemite (γ-Fe_2O_3), which have been intensively pursued for both fundamental scientific interests and technological applications in the last few decades (Wu et al,2010). Hematite is an n-type semiconductor with a band gap of 2.3 eV, where the conduction band (CB) is composed of empty d-orbitals of Fe^{3+} and the valence band (VB) consists of occupied 3d crystal field orbitals of Fe^{3+} with some mixture from the O 2p non-bonding orbital. As shown in figure 4 (a), Fe $^{3+}$ ions occupy two-thirds of the octahedral sites that are confined by the nearly ideal hexagonal close-packed O lattice.

2.4.2. Maghemite (γ-Fe_2O_3)

Maghemite (γ-Fe_2O_3), a typical ferromagnetic mineral (Zboril et al. 2002), is thermally unstable and is transformed to hematite at higher temperatures (Zborilet al. 2002). It has a spinel crystal structure which is similar to that of magnetite, except of vacancies in cation sub lattice. Two-thirds of the sites are filled with Fe (III) ions arranged regularly with two filled sites being followed by one vacant site. Maghemite (Υ-Fe_2O_3) as well as magnetite (Fe_3O_4) is easily magnetized and thus present high magnetic response when submitted to an external magnetic field (Cornell and Schwertmann, 2000). Maghemites are metastable oxides in the oxidative atmosphere and so they are oxidized to α-F_2O_3 when heated to a temperature above 673 K (Xu et al. 2008).

As shown in figure 4(c), the structure of γ-F_2O_3 is cubic; each unit of maghemite contains 32 O^{2-} ions, 21⅓ Fe^{3+} ions and 2⅓ vacancies. Oxygen anions give rise to a cubic close-packed array while ferric ions are distributed over tetrahedral sites (eight Fe ions per unit cell) and octahedral sites (the remaining Fe ions and vacancies). Therefore, the maghemite can be considered as fully oxidized magnetite, and it is an n-type semiconductor with a band gap of 2.0 eV.

2.4.3. Magnetite (Fe_3O_4)

Magnetite (Fe_3O_4) is a black mineral at room temperature which exhibits the strongest magnetism among the transition metal oxides (Teja and Koh, 2009). As shown in figure 4 (b), Fe_3O_4 has the face centered cubic spinel structure, based on 32 O ions and close-packed along the direction (Martinez et al, 2012). Fe_3O_4 differs from most other iron oxides in that it contains both divalent and trivalent iron or containing both ferrous (reduced) and ferric (oxidized) iron species, magnetite is often times described as iron $^{II, III}$oxide. Fe_3O_4 has a cubic inverse spinel structure that consists of a cubic close packed array of oxide ions, where all of the Fe^{2+} ions occupy half of the octahedral sites and the Fe^{3+} are split evenly across the remaining octahedral sites and the tetrahedral sites. In stoichiometric magnetite Fe^{II}/Fe^{III}= 1/2, and the divalent irons may be partly or fully replaced by other divalent ions (Co, Mn, Zn, etc). Thus, Fe_3O_4 can be both an n- and p-type semiconductor. Fe_3O_4 has the lowest resistivity among iron oxides due to its small band gap (0.1 eV) (Boxall et al, 1996). Fe_3O_4 nanoparticles has unique properties in nanoscale, such as a large surface area, high surface energy, low toxicity, good biocompatibility, super paramagnetic behavior, high absorption, and transfer electrons(Rahmawati R.,*et al,* 2018). The decreasing magnetite particle size should demonstrate reduced ferrimagnetic and enhanced super paramagnetic behavior. Similarly, increasing temperatures enhance thermal energy of particles and thus facilitate magnetic reorientation, or super paramagnetic magnetization.

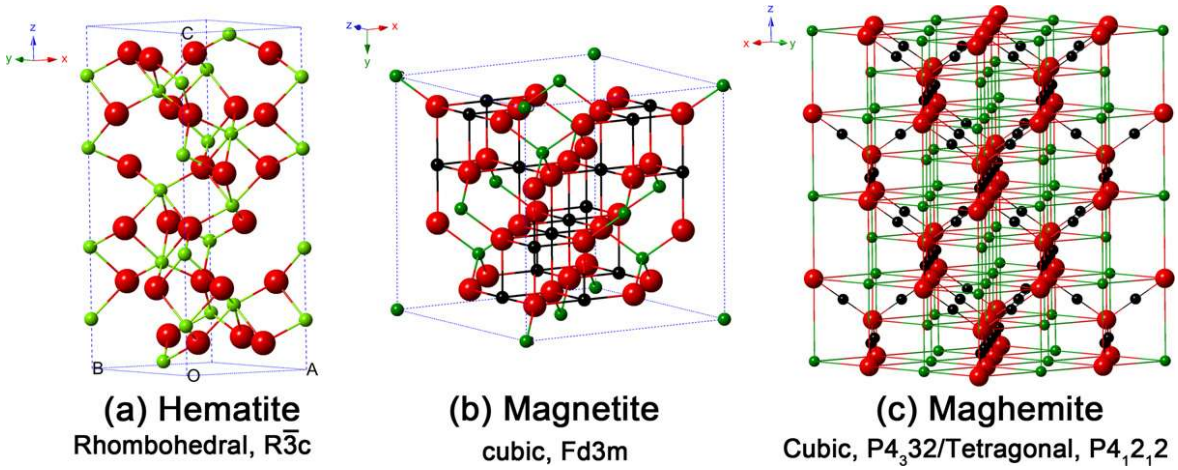

Figure 4: Crystal structure and crystallographic data of the hematite, magnetite and maghemite (the black ball is Fe^{2+}, the green ball is Fe^{3+} and the red ball is O^{2-}).

2.5. Surface Modification of Iron Oxide Magnetic Nanoparticles

Small particles tend to form agglomerates to reduce the energy related with the high surface area to volume ratio of the nanosized particles. Additionally, metallic nanoparticles have high chemical activity, and they are prone to oxidation in air, leading loss of dispersibility and magnetism. Thus, it is crucial for many applications to develop protection strategies for chemical stabilization of the naked magnetic nanoparticles against degradation during or after the synthesis. These strategies involve coating or grafting of with organic molecules, including (Wu.W etal, 2008) "small organic molecules or surfactants", polymers and "biomolecules or coating with an inorganic layer" such as silica, metal or nonmetal elementary substance, metal oxide or metal sulfide. In many cases the protecting shells stabilize the magnetic iron oxide nanoparticles, and they can be used for functionalization (Wu W. et al, 2008). An inert silica coating on the surface of magnetite nanoparticles avoid their aggregation in liquid and enhance the chemical stability. Iron oxide nanoparticles can be coated with silica (Zhang, C, 2007). These coatings not only provide stability to the nanoparticles in solution but also help in binding various biological ligands to the nanoparticle surface. These nanoparticles have an inner iron oxide core with an outer metallic shell of inorganic materials.

2.5.1. Silica Coating

Recently, Fe_3O_4 nanoparticles (MNPs) have attracted much research interest for applications in biomedical fields. Due to the use of these nanoparticles in medical applications, Fe_3O_4 must be chemically stable, biocompatible and must have a high degree of dispersion in various liquid mediums at different pH values (Sonmez, M., *et al* , 2015). Thus, the most promising and favorable coating material proved to be silica, as it not only protects magnetic nanoparticles against oxidation and agglomeration at wide pH ranges, but also improves their chemical stability. Moreover, the surface of silica is often finished with a silanol group, which can react with various chemicals and silane coupling agents to conjugate with a variety of biomolecules and specific ligands. Thus, SiO_2 layers have good compatibility and hydrophilicity, indispensable properties for the use of these materials in biomedical applications.

At present, the Stöber method and microemulsion are the most common methods of coating the surface of Fe_3O_4 nanoparticles with silica (Sonmez, M., et *al,* 2015). As for the former method, the

silica shells are formed through the hydrolysis and condensation of silane precursor, such as tetraethyl orthosilicate (TEOS). Due to the high hydroxylation rate of TEOS, formation of large aggregates and polydisperse products is inevitable. The microemulsion method uses micelles, which limit and control the coating of Fe_3O_4 core with silica. In general, silica coating will increase the size of particles and the magnetic properties of composite NPs also will change (Mahmoudi, M., et al2011).

Kulkarni, S.A was reported the synthesized Fe_3O_4 Nps coated with SiO_2 using the co-precipitationmethod. The synthesized Nps magnetization measurements confirm that the samples are super paramagnetic in nature and SEM analysis clearly shows that with the increase of TEOS amount, particle size also increases. Results prove that in the case of using Fe_3O_4/SiO_2 nanoparticles, their size is uniform and almost monodisperse, compared to simple magnetite nanoparticles, which are agglomerated (Kulkarni, S.A., *et al*, 2014).

To synthesize iron nanoparticles coated with uniformly thick layers of silica, the method of microemulsion is required (also known as water in oil). The microemulsion method has three main components: water, oil and surfactant. Using the reverse microemulsion, magnetite nanoparticles coated with uniformly thick silica layers were synthesized. In this method, micelles or reverse micelles are used as mini-reactor, to control the deposition of silica layers on magnetic nanoparticles.

Silica has been exploited as a coating material for magnetic nanoparticles. Chemical stability, low coercivity, strong magnetization, and biocompatibility of the dispersed magnetic nanoparticles are necessary for all biomedical application of magnetic colloids. In principal, silica coated magnetite or maghemite nanoparticles, comply with these requirements (Morel A-L.et al, 2008). Usually, an inert silica coating on the surface of magnetite nanoparticles prevents their aggregation in liquid, improves their chemical stability, and provides better protection against toxicity (Lesnikovich A. E., 1990). Silica coating has many advantages. First, it protects nanoparticles from agglomeration. Second, it prevents undesired reactions. Third, stable nanoparticles are obtained by silica coating. Final advantage of silica coating is providing easy further surface modification.

2.6. Application of Iron oxide Nanoparticles

Among the researchers working in the field of nanotechnology, magnetic nanoparticles have attracted intense experimental activities because of their potential applications in a numerous different industries such as storage of information, ferrofluid, audio and video recording, bioprocess gas sensor, refrigeration systems, medical applications, magnetic resonance imaging, catalyst, magneto optic, and removal of heavy metals (Nazari et al., 2014).

2.6.1. Magnetite Nanoparticles in Wastewater Treatment

Water is the most essential compound on the earth for the human activities. Proving clean water is the prime requirement of the human being for their better health. Water pollution is increasing worldwide due to rapid growth of industry, increase human population, and domestic and agricultural activities which leads to the life time threatening. Nowadays, numerous adsorbents have been investigated for the efficiency contaminant removal from wastewater including magnetite. Magnetite has been used in precipitation/coagulation/adsorption wastewater since the last few decades. Oskay (2003) reported that magnetite can remove some metals in wastewater from industries and synthetic wastewater. The efficiency of using magnetite nanoparticles is affected by many factors such as amount of magnetite used, particle size of magnetite, contact time between magnetite and wastewater and pH value of the solution. Moreover, the magnetite nanoparticles synthesized at low temperature $6^{o}C$ with pH 9 could effectively remove heavy metals from low and high concentration of initial concentration of heavy metal depending on the magnetite nanoparticles dosage. However, at low pH value, only small percentage removal of heavy metals was observed due to competition of proton and heavy metals from the oxide surface site. Magnetite nanoparticles were chosen as absorbents because of the following main advantages. Small size magnetite provides a large surface area and highly active surface sites, which then lead to a very high magnetite, can easily be separated from the treated water by supplying an external magnetic field (Hu et.al., 2005).

2.6.2. Use of Fe_3O_4 Nanoparticles for Heavy Metal Removal

Heavy metal pollution in the environment and effects on human health is within the most important issues. In conventional technologies, heavy metal removal/remediation is provided expensive because of non-regenerable materials used and high costs. Adsorption processes are

being widely performed by several researchers for this purpose and various materials have been frequently used as adsorbent. Litrature reviewed magnetite Nps are effective as adsorbent materials for removal of different heavy metal ions like As(V), Pb(II), Cd(II), Cr(VI), from water/wastewater.

2.6.2.1. Removal of Chromium, Cr (VI) Metal Ion

Currently, there is a fast growing interest in using iron oxide nanomaterials for heavy metal removal. Magnetite NPs, maghemite NPs and mixtures of two NPs were extensively studied for Cr (VI) removal. Chromium is widely used in many industrial processes such as mining industry, metallurgical industry (steel, ferrous- and nonferrous alloys), refractories (chrome and chrome-magnetite), electroplating, tannery, timber treatment and some other chemical industries. Leakage, unsuitable storage and/or improper disposal practices are the main reasons for releasing the considerable quantities of chromium to the environment.

The maximum level of total chromium level in drinking water is set as 0.05 mg/L, by World Health Organization(WHO, 2011). Chromium, which is a standout among the most lethal metals, is commixed into river stream and ground water through the electroplating businesses, metal finishing, cowhide tanning and chrome plating. In the natural environment, Cr(III) is most immobile, less soluble and stable, whereas Cr(VI) is highly mobile, soluble and bioavailable. Major Cr (VI) species include $HCrO_4^-$, chromate (CrO_4^{2-}) and dichromate ($Cr_2O_7^{2-}$). Cr (III) is the dominant form of Chromium at low pH (<4). Cr (III) is biologically important (50–200 µg day-1) to the human body, in which itinfluences sugar and lipid metabolism in humans. On the other hand, hexavalent chromium (Cr (VI)) is highly toxic, teratogenic and mutagenic.

It can cause severe damages to the human health including, but not limited to, liver and kidney damage, producing lung tumors, severe diarrhea, allergic dermatitis, skin irritation, internal hemorrhages and respiratory problems. Since Cr (VI) causes a great threat to humans as well as animals, cleaning up this contaminant from soil and water is critical. Several methods are available for the decontamination of waterscontaminated with Cr (VI) compounds. Some of these methods are reduction followed by chemical precipitation adsorption, electro-kinetic remediation, membrane separation processes and biosorption. In the presence of electron donors, Cr (VI) can be reduced to Cr (III), which is less toxic. Recently, the use of nanosized magnetic

material as adsorbents has attracted increasing interest due to their high surface area and unique superparamagnetism. These properties lead to high adsorption efficiency, high removal rate of contaminants and easy and rapid separation of adsorbent from solution using magnetic field. The magnetic nanoparticles are reusable after magnetic separation, by removing the adsorbed toxic contaminants (Shen, Y.F, 2009). Therefore Fe_3O_4 Nps used to remove in effective manner.

2.6.3. Electronic devices

The application of magnetite nanoparticles in modern information technologies is due to their availability of ultra-high density magnetic data storage devices. One of the most prominently uses is for magnetic hard disk drivers (HDD).

2.6.4. Targeted Drug Delivery

Magnetic nanoparticles are used widely for drug targeting applications owing to its suitability. They can effectively and safely transfer the drug (with maximum loading) to a specific site. Drug targeting/delivering by nanoparticles or nanocapsules reduces dosage and minimizes side effects, ensures the pharmaceutical effects, protects drugs against degradation and enhances drug stability.

2.6.5. Hyperthermia

Magnetic induction hyperthermia, one of the therapies for cancer treatment, means the exposition of cancer tissues to an alternating magnetic field. Magnetic field is not absorbed by the living tissues and can be applied to deep region in the living body (Gupta, A.K., 2005). When magnetic particles are subjected to a variable magnetic field, some heat is generated due to magnetic hysteresis loss. The amount of heat generated depends on the nature of magnetic material and of magnetic field parameters. Magnetic particles embedded around a tumour site and placed within an oscillating magnetic field will heat up to a temperature dependent on the magnetic properties of the material, the strength of the magnetic field, and the frequency of oscillation and the cooling capacity of the blood flow in the tumour site. Cancer cells are destroyed at temperature higher than 43 ^{0}C; whereas the normal cells can survive at higher temperatures. Heat could be generated applying an appropriate magnetic field. The size of the magnetite crystals is sub micrometric, so the powders or bulk of these biomaterials have comparable properties. These

materials are not only biocompatible, but also bioactive and could be useful for bone tumor (Gordon RT., 1979).

2.6.6. Antimicrobial activity of Fe_3O_4 Nanoparticles

Bacterial infections are still a major cause of morbidity and mortality. Bacterial strains resistant to the antibiotics now in use have become a serious public health problem that increases the need to develop new bactericidal materials. Consequently, there is a strong demand for developing novel strategies and new materials that can cope with these serious issues. The emergence of nanotechnology has created many new antimicrobial options (Beyth, N. et al, 2015). The small size of the nanomaterial (NM) is very suitable for carrying out antimicrobial biological operations. Antimicrobial NM now in use (i.e., metal, metal oxide, and organic nanoparticles) shows a diversity of intrinsic and modified chemical composition properties. Most known antibacterial nanomaterials interact electrostatically with the bacterial membrane causing membrane disruption. Frequently, free radicals (ROS) are produced due to the NM-membrane interactions. These radicals may instigate secondary membrane damage, hinder protein function, cause DNA destruction, and result in excess radical production. The physicochemical properties of the particles including size, shape, chemical modification and coating, and mixture in various ratios with other nanoparticles and solvent used all affect greatly their antibacterial activity (Gatoo, M. A.et al, 2014).

Many antibacterial studies were made using different nanoparticles such as Ag Nps, MgO Nps, TiO_2 Nps, ZnO Nps, CuO Nps, Al Nps, Bi Nps, Fe_3O_4 Nps and carbon based Nps. The reason for the bactericidal activity is due to the presence of reactive oxygen species (ROS) generated by different nanoparticles (Prabhu Y.T et al, 2015).

According to (Ameer Azam etal, 2012) the nanosized particles of pure ZnO, CuO, and Fe_2O_3 were synthesized by the sol–gel combustion method. XRD and TEM results showed that ZnO nanoparticles were smallest (18 nm) in size compared to CuO (22 nm) and Fe_2O_3 (26 nm). Furthermore, the antibacterial activity of all the three synthesized nanomaterials was compared and varied considerably. The order of antibacterial activity was demonstrated to be the following: ZnO > CuO > Fe_2O_3 (Ameer Azam, et al, 2012).

Fe_3O_4 in its bulk form and Au are generally considered inert and lack antimicrobial properties. Interestingly, these materials can be modified to introduce antimicrobial properties when synthesized as nanosize particles. Microbiological assays have proved that surfaces modified using Fe_3O_4 nanoparticles demonstrate antiadherent properties and significantly reduce both Gram-negative and Gram-positive bacteria colonization(Anghel.A et al, 2014).

Fe_3O_4-NPsexhibit considerable antibacterial effects because of their specific features including their size and larger surfacearea which facilitates their interactions with criticallyimportant biomolecules inside the bacterial cell. Chemical interaction between hydrogen peroxide and membrane proteins or between the chemical produced in the presence of Fe_3O_4 nanoparticles and the outer bilayer of bacteria could be the reason for the antibacterial activity of hydrogen peroxide produced enters the cell membrane of bacteria and kills them. It is also noted that nanoparticles continue to be in interaction with dead bacteria once the hydrogen peroxide is generated; thus foiling further bacterial action and continue to produce and release hydrogen peroxide to the medium.

Fe_3O_4 NPs are used in biosensors, food preservation agents, antimicrobial agents, magnetic refrigeration and storage media, ferrofluids, anti-cancer agents, magnetic resonance imaging (MRI), targeted drug delivery, and cell sorting. The biological compatibility and magnetic properties nanoparticles make them attractive for applications in biomedical research (Chen et al, 2008).

3. MATERIALS AND METHODS

3.1. Apparatus, Instruments and Chemicals

3.1.1. Apparatus

The apparatus were used in this research work includes different sizes of beakers, conical flask, round bottom flask, funnels, volumetric flasks, droppers, spatula, measuring cylinder, reagent bottle, mortar, filter paper, crucible dish, magnetic stirrer, magnet, and tong.

3.1.2. Instruments

The instruments were used in the study includes:electronic analytical balance, Hot plate, Drying oven, FT-IR spectrometry (FT-IR, Perkin Elmer-65), X-ray powder diffractometer (XRD 7000, shimadzu), Thermogravimetry-Differential thermal analyzer (DTG-60H, Shimadzu Co., Japan) and Field emission scanning electron microscope (FE-SEM).

3.1.3. Chemicals and Reagents

The chemicals were used for the synthesis of Fe_3O_4 Nps and silica coated Fe_3O_4 Nps: Iron (III) nitrate nonahydrate($Fe(NO_3)_3.9H_2O$, 98% Sigma Aldrich), Iron (II) sulfate heptahydrate ($FeSO_4 \cdot 7H_2O$,98·5% Sigma Aldrich), ammonia (25% NH_3, ultra pure, France, Carlo Erba), Polyoxyethylene sorbitan monooleate (Tween-80), Sodium Dodecyl sulphate, (SDS), 1-butanol (CH_3 $(CH_2)_3OH$,99.5%, Ranchem India), n-heptanes (C_7H_{16} ,99%, Ranchem India), silicon oxide (SiO_2), acetone and distilled water. All the chemicals are analytical grade and were used without further purification.

3.2. Synthesis of Fe_3O_4 Nanoparticle by Microemulsion

3.2.1. Preparation of Fe_3O_4 nanoparticle using Tween-80

The Fe_3O_4 magnetic nanoparticles can be prepared by water-in oil micro-emulsion method that reported by Xuan Nui Pham et al (2016) but with some modification. The microemulsion system used in this study consisted of tween-80 as the surfactant, 1-butanol as the co surfactant, n-heptanes as the continuous oil phase and an aqueous solution of reactants as the dispersed phase. The ratio of surfactant to co-surfactant was fixed at 1:1 on the volume basis i.e. 20 ml of tween-80/butan-1-ol and 60ml n-heptanes.

The precursor solution (solution A) contains 2:1 mole ratio of iron salts (20 ml of 0.4 M Fe $(NO_3)_3.9H_2O$) and(20 ml of 0.2 M $FeSO_4.7H_2O$) was dissolved in 80 ml mixture of tween-80/butan-1-ol/n-heptanes. This results in the formation of a reverse micro-emulsion. Mixture B contains 80 ml of tween-80/butan-1-ol/n-heptanes was added to aqueous NH_3 (50 ml of 25% aqueous NH_3). These solutions were stirred with speed of 300 rpm for 30 min at room temperature. Mixture B was added to solution A and the combined mixture was stirred continuously with a rotational speed of 1000 rpm for $2\frac{1}{2}$hr at different temperatures of 30, 50, and 80°C. The magnetic nanoparticles can be separated by magnetic force and washed several times by distilled water and acetone to eliminate the ammonia and the surfactant. Finally, the magnetic Fe_3O_4 nanoparticles was obtained after drying in a vacuum oven and recorded as Fe_3O_4-30T, Fe_3O_4-50T, and Fe_3O_4-80T, respectively and kept for characterization and further use. Fe_3O_4 nanoparticles were synthesized also from precursors with different concentration to study its effect on nanoparticle size. The chemical reaction of Fe_3O_4 formation is written as following equation (Gholami,A., 2016).

$$Fe^{2+} + 2Fe^{3+} + 8OH^- \longrightarrow Fe_3O_4\ (black) + 4H_2O$$

3.2.2. Preparation of Fe_3O_4 Nanoparticle using SDS

Fe_3O_4 Nps was synthesized by using the same amount and type of precursor, oil phase and base and following the same procedure in section 3.2.1 with surfactant SDS.

3.2.3. Preparation of Silica coated Fe_3O_4 Nanoparticles using tween-80

Silica-coated Fe_3O_4 nano particles were prepared in similar manner with section 3.2.1 except that mixture B (ME2) contained neat 10 ml of 0.2M SiO_2 aqueous solution and performed at 30^oC temperature.

3.3. Characterization Techniques

3.3.1. Thermal Gravimetric Analysis (TGA)

Thermal gravimetric analysis (TGA) was carried out using a simultaneous DTA-TG apparatus (DTG-60H, Shimadzu Co., Japan) to determine the thermal stability of the synthesized material. Approximately 15.59 mg of the Fe_3O_4 nanoparticle samples were placed in a platinum crucible

on the pan of the microbalance and heated from room temperature to 800°C, using Al_2O_3 as inert material.

3.3.2. XRD Study

X-ray diffraction patterns for the synthesis nanoparticles were recorded using a BRUKER D8 Advance X-ray diffractometer equipped with a Cu target for generating a Cu Kα radiation (wavelength 1.5406 Å) as the X-ray source. The measurements were made at room temperature and the accelerating voltage and the applied current were 40 kV, 30mA, respectively. The instrument was operated under step scan type with step time and degree (2θ) of 0.4s and 0.020°, respectively, over 10° to 80°,to determine the crystal structure of the samples. The crystal size of NPs was determined from the XRD pattern by using Debye-Scherer's equation that is mentioned in equation 2.

3.3.3. Fourier Transform Infrared (FT-IR) Study

Fourier transformer infrared spectroscopy (FTIR) spectra of the micro emulsion synthesized Fe_3O_4 nanoparticles and silica coated Fe_3O_4 nanoparticles was recorded at room temperature using a FTIR spectrophotometer in order to analyze and detect surface functional groups in the scanning range of 4000 – 400 cm^{-1}.The FTIR spectra were obtained from pellets of the synthesized powder mixed with potassium bromide (KBr) by using a Perkin Elmer 65 Spectrum of spectrophotometer. A milligram of each sample was mixed and crushed with about 0.2 g of dried KBr. The samples were formed into pellets 13 mm in diameter and 0.5 mm in thickness by mould pressing. The FTIR measurements were performed on the pellets placed in a window of IR radiation with measurements recorded between 4000 - 400 cm^{-1} at a resolution of 4 cm^{-1}. FTIR spectra yield information on the chemical bonds between the Fe_3O_4 core and the organic surface coverage. This method identifies materials by the "fingerprints" of molecules, as each FTIR spectrum is unique to the measured molecule.

3.3.4. Scanning Electron Microscopy Study

SEM reveals information about the sample including external morphology, chemical composition and crystalline structure and orientation of materials making up the sample. For SEM characterization, nanoparticles solution should be first converted into a dry powder, which

is then mounted on a sample holder followed by coating with a conductive metal, such as gold, using a sputter coater. The sample is then scanned with a focused fine beam of electrons. The surface characteristics of the sample are obtained from the secondary electrons emitted from the sample surface.

3.4. Methods of Antimicrobial Test

Materials which were used for antimicrobial activities are Muller-Hinton agar, DMSO, petriplates, para film tape, incubator, Fe_3O_4 nanoparticle and silica coated Fe_3O_4 nanoparticles sample, Gram- negative and Gram-positive bacteria and C.ablicans fungi.

3.4.1. Preparation of Inoculums

Nutrient broth (1.3 g in 100 mldistilled water) was prepared in 5 conical flasks and sterilized. In the first conical flask clinically isolated strain of *Staphylococcus aureus* and in the second conical flask clinically isolated strain of *Bacillus subtilis* were inoculated. In the third conical flask clinically isolated strain of *Escherichia coli* and *Pseudomonas aeruginosa* in the fourth conical flask clinically isolated strain ofwere added and in the 5^{th} conical flask C.ablicans fungi was inoculated. Microbial cultures inoculated in nutrient broth will be kept on rotary shaker for 24 hours at 100 r.p.m.

3.4.2. Agar Well diffusion Method

Antimicrobial testing was performed against Gram-negative (*Escherichia coli* and *Pseudomonas aeruginosa*) and Gram-positive (*Staphylococcus aureus* and *Bacillus subtilis*) bacteria and Candida ablicans fungi. Microbial strains are obtained from ASTU biology laboratory that is obtained from pastor institute. Microbial cultures were maintained on nutrient Muller-Hinton agar at 37^0C and the cultures were kept in appropriate media slants and stored at 4^0C until used. The antibiotic gentamicin was used as a positive control and DMSO as anegative control in this study. The antimicrobial activity of the different concentration of Fe_3O_4 and silica coated Fe_3O_4 Nps was evaluated by Agar well diffusion method adopted by (Nitha*et al*, 2012) but with some modification. Sterile nutrient plates were prepared. The plates were allowed to solidify for 5 minutes and wells of 6mm were punctured in selected areas on different plates using a well borer. 1mL inoculums suspension of Gram-negative (*Escherichia coli* and *Pseudomonas*

aeruginosa) and Gram-positive (*Staphylococcus aureus* and *Bacillus subtilis*) and C.ablicans were swabbed uniformly over the surface of the agar plate. 100 mg and150 mg uncoated Fe_3O_4 and silica coated Fe_3O_4 nanoparticles were dissolved in10 mL and 15 mL DMSO respectively, to obtain each 10 mg/mL and 15 mg/mL Then, 100 µL of each prepared Nps was loaded into the well and the plates were kept for incubation at 37ºC for 24 hours. The antimicrobial activity was evaluated in terms of zone of inhibition, measured and recorded in millimeters using ruler. Clear inhibition zones formed around the well indicated the presence of antimicrobial activity.

4. RESULTS AND DISCUSSION

4.1. Characterization of Prepared Nanoparticles

4.1.1. Thermogravimetry differential thermal analysis

The thermal properties of Fe_3O_4 were investigated by analytical techniques of TG-DTA. Measurement was conducted at a heating rate of 15°C min^{-1} up to 800°C. Figure 5 shows the thermo gravimetric analysis (TGA) and differential thermal analysis (DTA) of the Fe_3O_4 nanoparticles. TGA curve shows mass loss of the sample where as DTA curve indicates the energy gain or loss during the process.The Fe_3O_4 nanoparticles were thermally stable and there was no essential weight loss over the entire temperature range in TG curve (Figure 5). The total weigh lose as shown in TG curve exhibited only 3.726% weight loss, where the largest portion of these weight losses occurred at the temperatures of 25–250°C. Hence, this weight loss is related to removal of the physically adsorbed water and/or hydroxyl groups on the surface of Fe_3O_4 nanoparticles. At higher temperature there is no significant change of weight. This implies the surfactant and co-surfactants were removed through washing from the as-synthesized Fe_3O_4 Nps and not need calcinations for the materials that synthesized by microemulsion method.

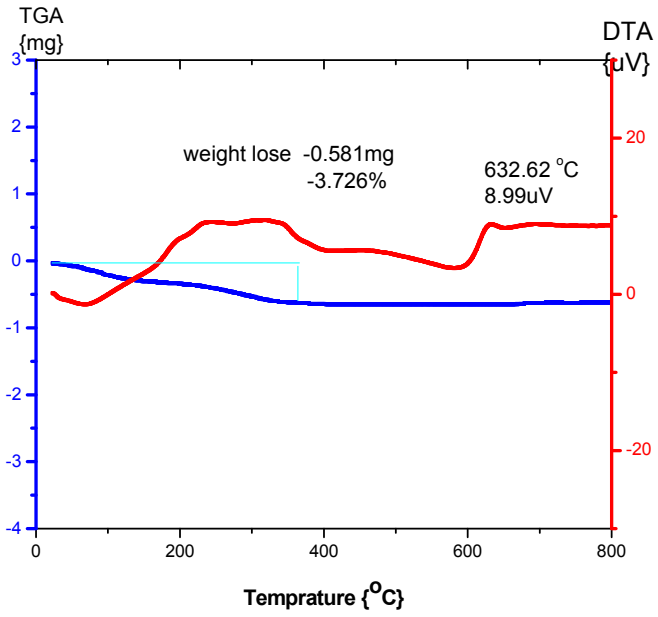

Figure 5: TG-DTA curves for Fe_3O_4 nanoparticles using Tween-80 surfactant at 30°C

4.1.2. X-ray Diffraction

Figure 6 illustrates the XRD patterns of iron oxide nanoparticles synthesized by micro-emulsion method using tween-80 surfactant at different temperatures (30°C, 50°C and 80°C).

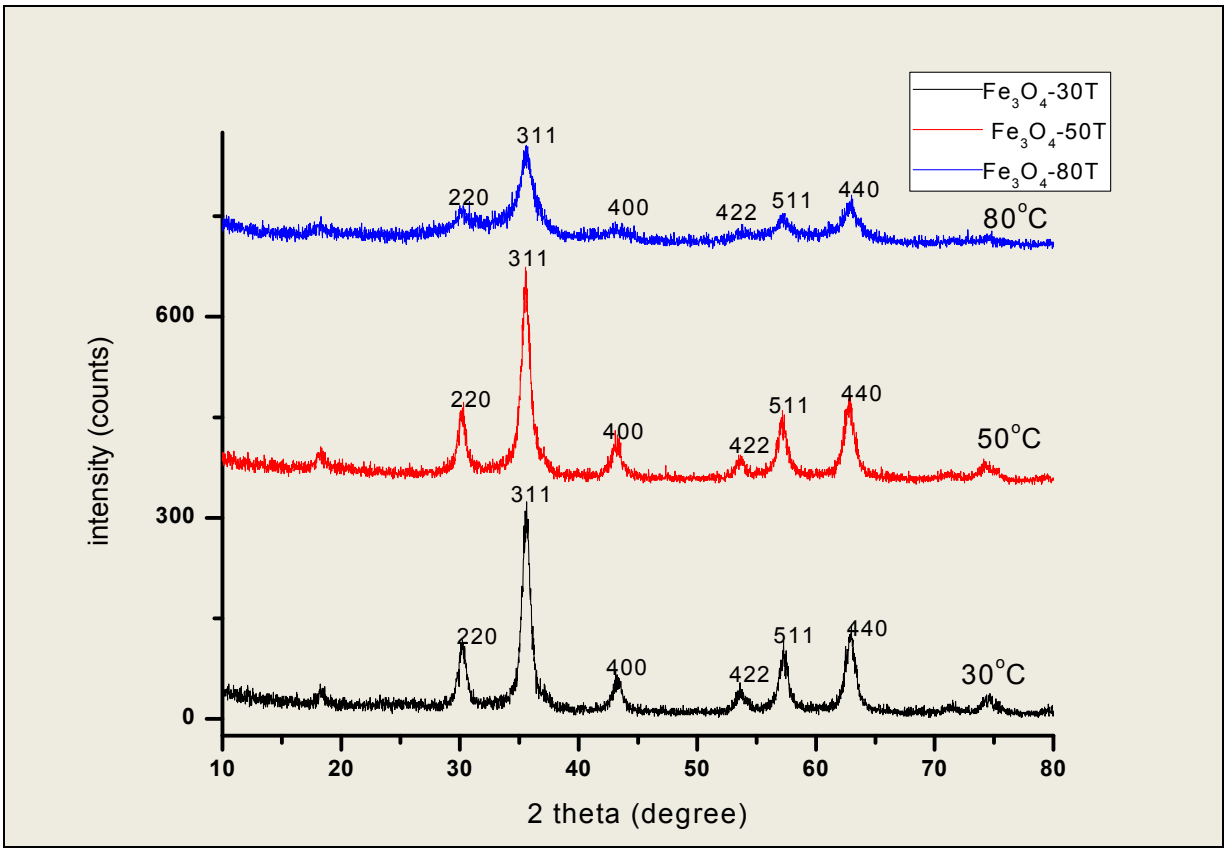

Figure 6: XRD patterns of Fe_3O_4 nanoparticles using Tween-80 surfactant at different temperatures

The Fe_3O_4 diffraction patterns have main peaks at 2θ values of 30.2°, 35.6°, 43.2°,53.56, 57.2°, and 62.8° corresponding to the reflection from (220), (311), (400) ,(422) (511), and (440) crystal planes. The position and relative intensity of all diffraction peaks match well with those of the magnetite (JCPDS Card. No. 79-0418) and the narrow sharp peaks of materials indicate that the nanoparticles have relatively high crystallinity and without the appearance of the impurities phase of goethite α-FeO(OH) and hematite (Fe_2O_3) corresponding to the diffraction peaks of (110), (104) at 2θ positions of 21.22° and 33.15. The particle size is determined by taking the average of the sizes at the peaks D_{220}, D_{311}, D_{400}, D_{511} and D_{440}. The broadening of Bragg's peaks

indicates the formation of nanoparticles. The calculated mean crystallite size of the Fe_3O_4 nanoparticles synthesized by micro-emulsion method using tween-80 surfactant with three different temperatures 30°C, 50°C and 80°C was about 7.85 nm, 8.41 nm and 10.83 nm, respectively. The lattice parameter "a" and interplanar spacing $d_{h\,k\,l}$ are determined by Equation (3).

$$\lambda = 2d \sin(\theta)$$

$$d_{h\,k\,l} = \frac{a}{\sqrt{h^2+k^2+l^2}} \quad \text{.....3}$$

The crystal structure of the nano-Fe_3O_4 particles belongs to cubic system with lattice parameters (a = 8.354, 8.366 and 8.356 Å at three different temperatureusing d-spacing 2.51887, 2.52261 and 2.5199 respectively for the miller index of major peak D_{311}.

Table 2: The average crystallite size of samples of Fe_3O_4 nanoparticles from XRD using Tween-80 surfactant

Sample	Temp (^oC)	h kl	2 theta	Cos ɵ	FWHM	B(rad)	D	Lattice parameter(a)
Fe_3O_4-30T Nps	30	220	31.2418	0.963	0.92	0.016049	8.69	8.354
		311	35.614	0.952	1.26	0.02198	6.67	
		400	43.1068	0.93	0.89	0.015526	9.22	
		511	57.2053	0.878	0.96	0.016747	8.07	
		440	62.8334	0.8534	1.14	0.019887	6.61	
Average size							7.85	
Fe_3O_4-50T NPs	50	220	30.183	0.9655	0.82	0.014304	9.77	8.366
		311	35.5594	0.952	0.9	0.0157	8.78	
		400	43.1818	0.93	0.92	0.016049	8.39	
		511	57.1553	0.878	0.94	0.016398	7.75	
		440	62.8734	0.8537	0.963	0.016799	7.36	
Average size							8.41	
Fe_3O_4-80T Nps	80	220	30.2446	0.9654	0.8167	0.014247	9.81	8.357
		311	35.5989	0.952	0.8767	0.015294	9.01	
		400	43.2667	0.9296	0.4	0.006978	19.28	
		511	57.2353	0.8823	0.86	0.015002	8.51	
		440	62.8734	0.853	0.94	0.016398	7.53	
Average size							10.83	

Since the lattice parameter and particle size almost similar for Fe_3O_4 Nps synthesized at different temperature. As a result room temperature synthesis of the material is possible by the method selected.

Diffraction patterns of the Fe_3O_4 synthesized using SDS at different temperatures (30^oC, 50^oC, 80^oC) are $2\Theta = 30.3^o$, 35.58^o, 43.33^o, 53.6^o, 57.34^o, 62.86^o corresponding with the miller indexes 220, 311, 400, 422, 511 and 440 respectively, which are the characteristic peaks of the Fe_3O_4

crystal with a cubic spinel structure. It is clear that the phase of XRD pattern match with Fe_3O_4 Nps according to JCPDS card no 00-019-0629. The synthesis Fe_3O_4 Nps poorly crystalline when compared with obtained using Tween-80 surfactant. With the XRD pattern as it is mentioned above, the average diameter which can be evaluated from Scherrer equation. ($D = K\lambda / \beta\cos\theta$, where K is constant, λ is X-ray wavelength and β is the peak width of half-maximum) is given in Table 3.

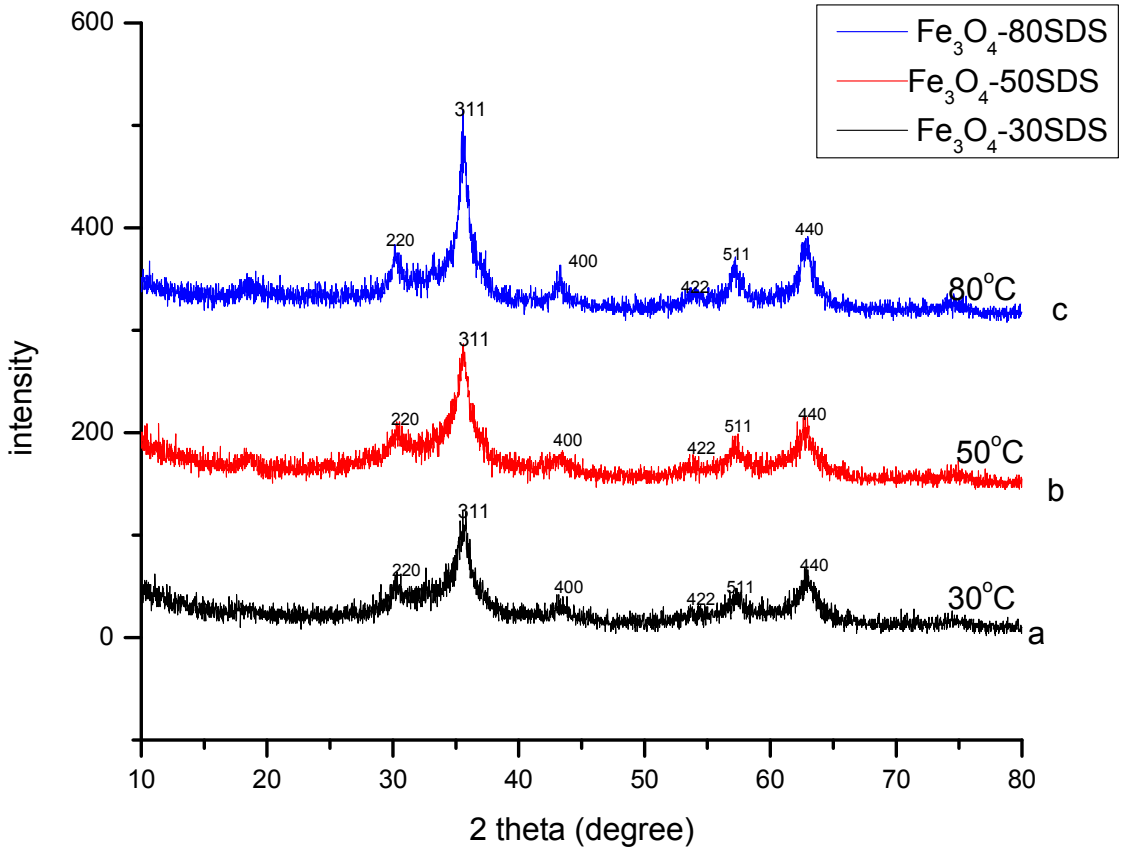

Figure 7: XRD patterns of Fe_3O_4 nanoparticles using SDS surfactant at temperatures 30°C, 50°C and 80°C

Table 3: The crystallite size of the Fe_3O_4 nanoparticles synthesized by micro-emulsion method using SDS surfactant

Sample	Temp (°C)	h kl	2 theta	Cos Θ	FWHM	B(rad)	D	(a)
Fe_3O_4-30TSDS Nps	30	220	30.3029	0.965	0.64	0.011164	12.51	8.361
		311	35.5824	0.9523	1.25	0.021806	6.32	
		400	43.3317	0.9294	1.12	0.019538	6.89	
		511	57.3403	0.9744	0.87	0.015177	9.29	
		440	62.8634	0.8533	1.32	0.023027	5.36	
Average size							8.07	
Fe_3O_4-50SDS Nps	50	220	30.3029	0.965	0.88	0.015351	9.10	8.355
		311	35.6073	0.9521	1.18	0.020584	6.70	
		400	43.2917	0.929	0.84	0.014653	9.18	
		511	57.0953	0.8784	0.82	0.014304	8.89	
		440	62.7609	0.8537	1.075	0.018753	6.60	
Average size							8.1o	
Fe_3O_4-80SDS Nps	80	220	30.243	0.9654	0.76	0.013258	10.54	8.352
		311	35.6223	0.9521	0.99	0.01727	7.98	
		400	43.1918	0.9298	0.52	0.009071	14.84	
		511	57.2203	0.8779	0.99	0.01727	7.36	
		440	62.8184	0.8535	1.09	0.019014	6.50	
Average size							9.44	

Effect of reaction temperature

Reaction temperatures at 30°C, 50°C and 80°C were tested, while other preparation conditions were the same to investigate effect of temperature. The mean crystallite size of the Fe_3O_4 nanoparticles synthesized by micro-emulsion method using tween-80 surfactant with three different temperatures 30°C, 50°C and 80°C were about 7.85, 8.41 and 10.83 nm, respectively and the calculated mean crystallite size of the Fe_3O_4 nanoparticles synthesized by micro-emulsion method using SDS surfactant with three different temperature 30°C, 50°C and 80°C were 8.07

nm, 8.1 nm and 9.44 nm respectively. In both cases as indicated in Table 2 and 3 the particle size slightly increases with temperature rising. The reaction temperature change for such method does not favours large particle formation.

The temperature is an important factor to be considered in the synthesis of magnetite nanoparticles. It is a factor that influences strongly the nucleation and growth mechanisms (Cai, Wei et al, 2007). When the temperature increases, the particle size becomes bigger and particle size distribution shows irregular shapes. The increase in frequency of collision between the particles leads to kinetic energy of collision increasing, this makes the nano-particles have strong tendency to overcome potential barrier between them, and agglomerate into large particles, as a result, a phenomenon of agglomeration takes place.

Effect of concentration of Fe^{3+} and Fe^{2+}

Fe_3O_4 nanoparticles were prepared with different concentrations of Fe^{2+},Fe^{3+} in aqueous phase, and other preparation conditions were the same to investigate effect of concentration precursor. The concentration of the precursor has a major influence on size of nanoparticles. It has some effect on the size as high concentration favors larger nanoparticle size (Sibokoza, S. B et al, 2017). Figure 8 showed the XRD pattern ofFe_3O_4 nanoparticles by varying precursor concentrations. It was found that the size of nanoparticles were 7.3, 8.6 and 10.3 nm from the X-ray line broadening that is given in table 4.

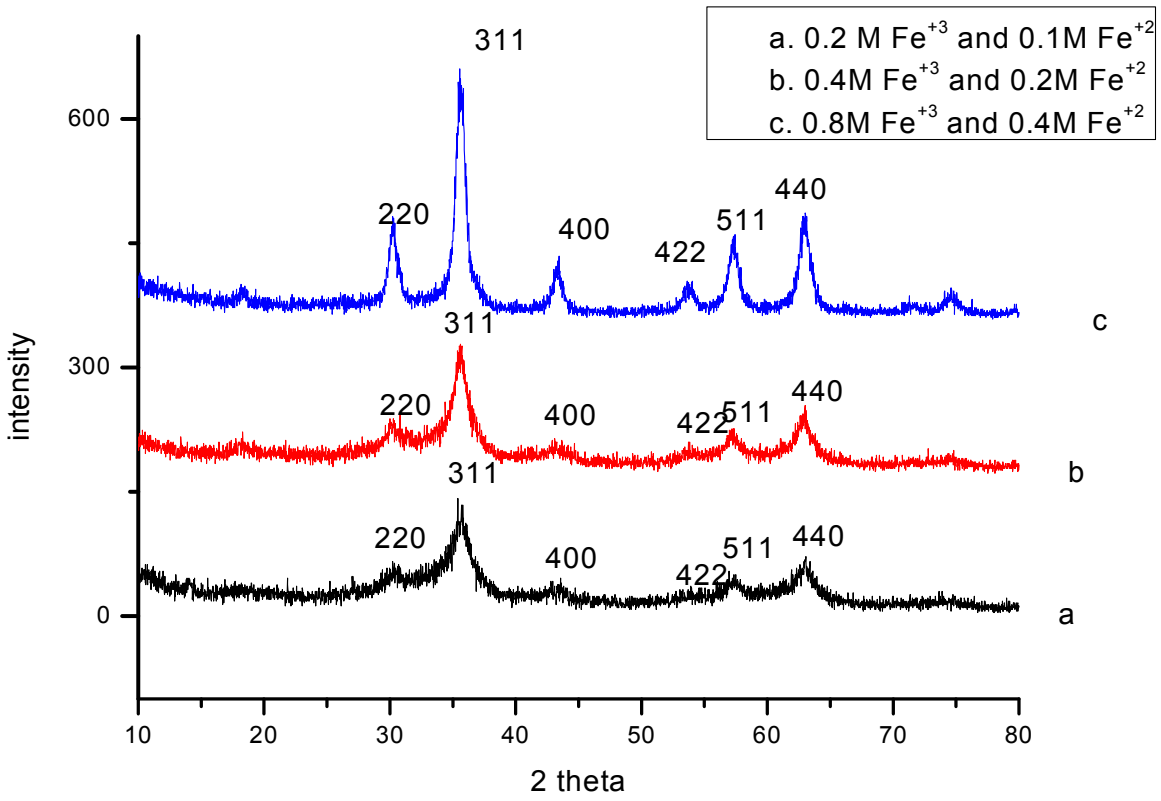

Figure 8: XRD patterns of Fe_3O_4 nanoparticles at 30^{o}C by varying precursor concentration

As shown in Table 4 when the concentration of precursor change from 20 ml of 0.4 M Fe^{+3} and 20 ml of 0.2 M Fe^{+2} to 20 ml of 0.2 M $Fe^{+3}$and 20 ml of 0.1M Fe^{+2} the Fe_3O_4 Nps size decrease from 7.85 to7.5 and when the concentration precursor change from 20 ml of 0.4 M Fe^{+3} and 20 ml of 0.2 M Fe^{+2} to 20 ml of 0.8 M $Fe^{+3}$and 20 ml of 0.4 M Fe^{+2} the Fe_3O_4 Nps size increase from 7.85 to 8.64 nm. The size of nanoparticles was found to increase in precursor concentration resulted in an increase in nanoparticle size.

Table 4: The crystallite size of the Fe_3O_4 nanoparticles synthesized by micro-emulsion method using tween-80 surfactant by varying precursor concentration

Precursor concentration	h kl	2 theta	Cos Θ	FWHM	B(rad)	D	Lattice parameter(a)
0.2M Fe^{+3} and 0.1 M Fe^{+2}	220	30.4528	0.965	0.9	0.0157	8.90	8.342
	311	35.6656	0.952	1.6367	0.028551	4.83	
	400	43.6515	0.928	0.64	0.011164	12.03	
	511	57.9565	0.8775	0.96	0.016747	7.59	
	440	62.9234	0.853	1.52	0.026516	4.66	
Average size						7.5	
0.4M Fe^{+3} and 0.2 M Fe^{+2}	220	31.2418	0.963	0.92	0.016049	8.69	8.354
	311	35.614	0.952	1.26	0.02198	6.67	
	400	43.1068	0.93	0.89	0.015526	9.22	
	511	57.2053	0.878	0.96	0.016747	8.07	
	440	62.8334	0.8534	1.14	0.019887	6.61	
Average size						7.85	
0.8M Fe^{+3} and 0.4 M Fe^{+2}	220	30.2596	0.965	0.7667	0.013375	10.44	8.349
	311	35.6348	0.952	0.915	0.015962	8.63	
	400	43.3067	0.929	0.87	0.015177	8.86	
	511	57.2753	0.878	0.94	0.016398	7.75	
	440	62.9334	0.853	0.94	0.016398	7.53	
Average size						8.64	

Figure 9 shows XRD pattern of silica coated Fe_3O_4 magnetic nanoparticle. It is seen the silica coated Fe_3O_4 NPs exhibit diffraction patterns similar to that of Fe_3O_4 NPs. The diffraction peaks at 30.2^o, 35.6^o, 43.3^o, 53.8^o, 57.3^o, and 63^o refer to (220), (311), (400), (422), (511), and (440) planes of cubic inverse spinel Fe_3O_4, respectively. The additional Peak at 26.6^o and 51.1^o degree corresponds to SiO_2 (Yunusa, S., et al, 2016) and the rest of peaks are as those in XRD patterns of Fe_3O_4.

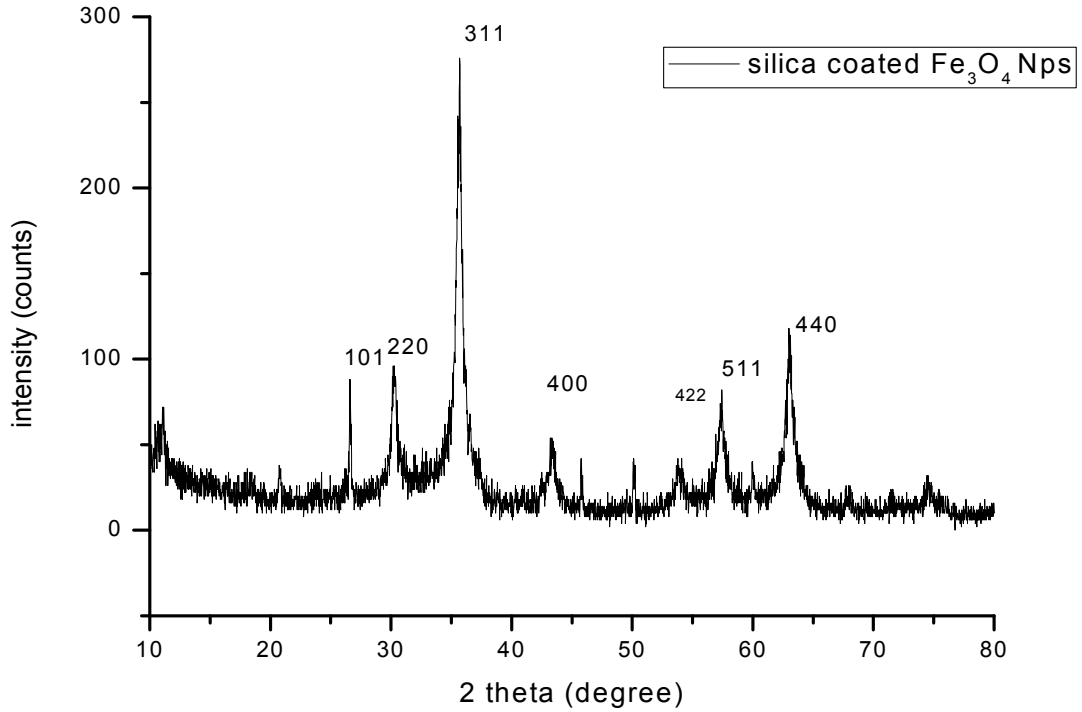

Figure 9: XRD pattern of silica coated Fe_3O_4 Nps

The average crystal size of silica coated Fe_3O_4 obtained by calculation of Sharer's formula, is about 16 nm using the peaksD_{220}, D_{311}, D_{400}, D_{511} and D_{440}.

Table 5: The calculated mean crystallite size of the silica coated Fe_3O_4 nanoparticles

Sample	Hkl	2 theta	cosϴ	FWHM	ß(rad)	D	Lattice parameter(a)
silica coated Fe_3O_4	220	30.213	0.965	0.48	0.008373	17.87	8.349
	311	35.663	0.952	0.5886	0.010268	14.8	
	400	43.3367	0.929	0.59	0.010292	15.15	
	511	57.3453	0.8774	0.6	0.010467	15.74	
	440	63.0016	0.8526	0.5833	0.010175	16.68	
	average size					16	

The average crystalline size of silica coated Fe_3O_4 NPs was found to be 16 nm. As shown from the Table 5 silica coated Fe_3O_4 nanoparticles have greatter crystalline size than uncoated Fe_3O_4 nanoparticles. The increase in crystal size may be due to the addition of large amount of SiO_2. Similar result reported by Sachnin A. Kulkarni that the particle size is increased with the increase in tetraethyl orthosilicate content.

4.1.3. FTIR spectra analysis

Figure 10 demonstrates the FT-IR spectrum of Fe_3O_4 nanoparticles synthesized using Tween-80 and SDS as surfactant as well as the silica coated Fe_3O_4 Nps. Since Fe_3O_4 Nps has an inverse spinel-type structure, it shows bands indicating the vibrations M_T–O–M_O ($v1 \approx 600–550$ cm^{-1}) and M_O–O ($v_2 \approx 440$-470 cm^{-1}) where M_t and M_o correspond to the metal occupying tetrahedral and octahedral positions, respectively (Andrade A. L. et al, 2009). In Figure 10 a, the peaks at 3421cm^{-1} and 2348 cm^{-1} indicate the presence of OH and C=O respectively, probably due to atmospheric moisture and CO_2 respectively. The presence of two strong absorption bands of all materials at around 636 and 588 cm^{-1} shows the formation of magnetic nanoparticles. Moreover, the band at 588 cm^{-1} was confirmed as the Fe-O stretching vibration of tetrahedral sites of spinel structure and the absorption bands at 445 cm^{-1}, attributed to tetrahedral and octahedral sites (Prabhu, Y.T., 2015).

FT-IR spectrum shows less intense H-O-H bending vibration in the region 1623 - 1089 cm^{-1}, typical of the H_2O molecule. These peaks values nearly matches with the reported values of Kim et al 2007.

Fig. 10 b shows the typical FTIR spectrum of the pure Fe_3O_4 nanoparticles synthesize using SDS surfactant. Two absorption bands at 585 and 442 cm^{-1} corresponding to the Fe–O bonds in tetrahedral and octahedral sites confirm the spinel type structure of pure Fe_3O_4 nanoparticles (Mandal, M. *et al*, 2005). The FTIR spectra of pure Fe_3O_4 nanoparticles also exhibit absorption bands appearing at 1623cm^{-1}, which can be attributed to hydroxyl groups that cover the surface of Fe_3O_4 nanoparticles due to aqueous media synthesis. The peak at 3401 cm^{-1} was the characteristic of stretching vibration of OH.

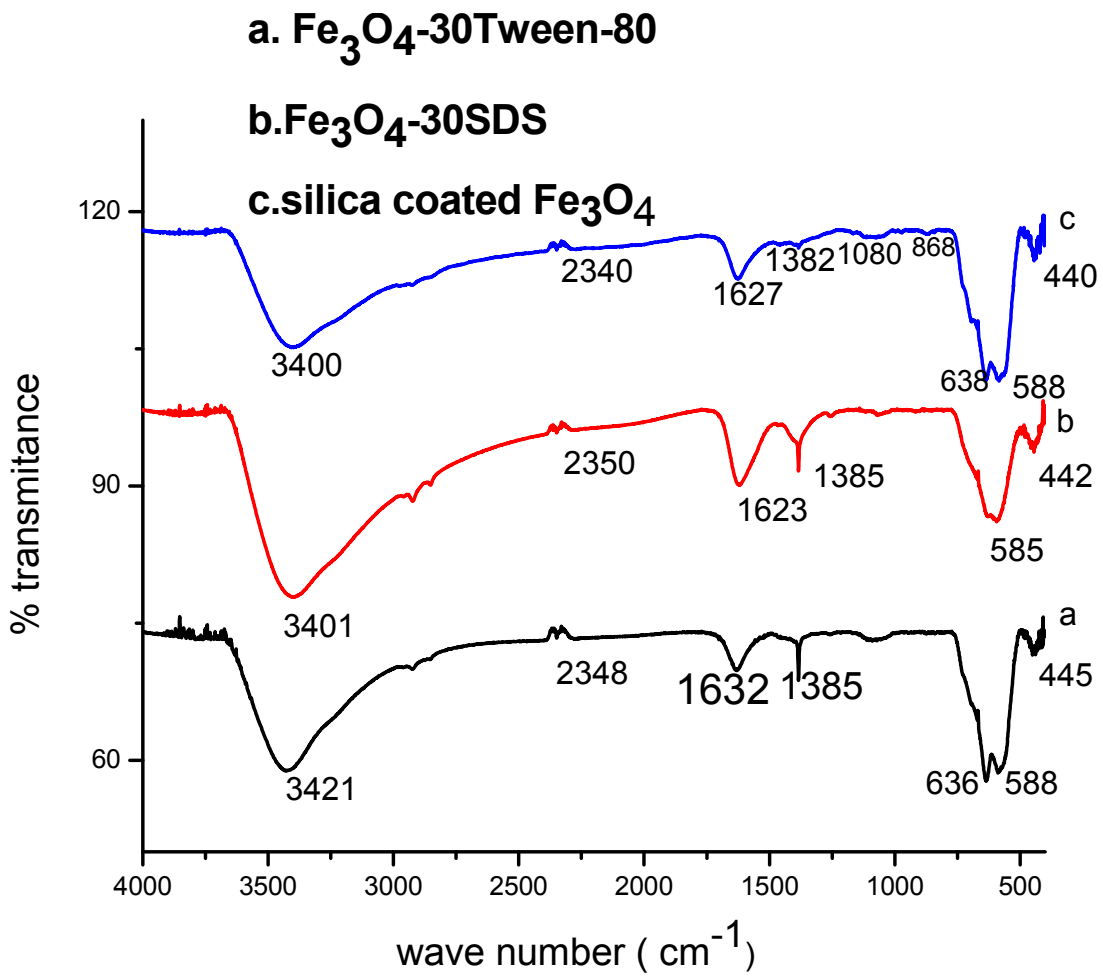

Figure 10:FTIR spectrums of Fe_3O_4 Nps using a. tween-80 surfactant b. SDS surfactant c. silica coated

Figure 10 c, with absorption peak at 588-638cm^{-1} confirming the presence of a Fe–O bond related to the magnetite phase of magnetite nanoparticles. FT-IR spectrum showed bending vibration in the region 1627 - 1382 cm^{-1}, typical of the H_2O molecule. Bands at 868 cm^{-1} and 1080 cm^{-1} were due to symmetric and asymmetric linear vibrations of Si–O–Si, indicative of formation of a silica shell with SiO_2-modified magnetite (Silvia Villa et al, 2016). This data supports the formation of SiO_2 shell on Fe_3O_4 nanoparticles. The transmittance of coated Fe_3O_4 NPs was slightly lower than that of Fe_3O_4 NPs because of coating**.**

4.1.4. Surface morphology Analysis

The morphology of Fe_3O_4 nanoparticles and silica coated Fe_3O_4 Nps was studied using SEM images. The surface morphology of the synthesized samples was viewed through the high

resolution field emission scanning electron microscope (FE SEM). The images were obtained at 2.00 kV of accelerating voltage using 8.3 mm working distance at different magnification. Figure 11 (a, b) show the SEM image of Fe_3O_4 nanoparticles synthesis using tween-80 surfactant, it can be seen clearly that the particles are homogenously distributed with some agglomerates and their size distributions of particles were in the range of 17.69 to 33.36 nm and at high magnification, it has flower like shape (Fig. 11b). The mean diameter of the nanoparticles was 24 nm which is deviate from the size calculated by the Debye–Scherrer formula due to agglomeration. Thus, the nanoparticles were successfully prepared also confirm by SEM.

Figure 12 (a, b) shows the SEM images of Fe_3O_4 nanoparticles synthesis using SDS surfactant, still agglomerated profound. The size distributions of particles were in the range of 17.69 to 30.07 nm. The mean diameter of the nanoparticles was 25.9 nm. Almost all particle size of Fe_3O_4 nano particles is below 26 nm. Figure 13 shows the SEM image of silica coated magnetite nanoparticles. It showed that the nanoparticles were homogeneous and without any substantial agglomeration. Coating the surface of magnetic nanoparticles with suitable and nontoxic compounds has been proven to be one of the most efficient ways for providing stability of the nanoparticles. On the other hand agglomeration of naked Fe_3O_4 nanoparticles due to the vander-waals force between the particles reduces after surface modification. The size distributions of particles were in the range of 34.39 to 37.3 nm which exhibit a relatively narrow size distribution. From the FE-SEM image mean diameter silica coated Fe_3O_4 nanoparticles was calculated as 35.3 nm, which was bigger than the XRD report which is related to the dry state of the XRD measurement (Asgari S.et al, 2014).

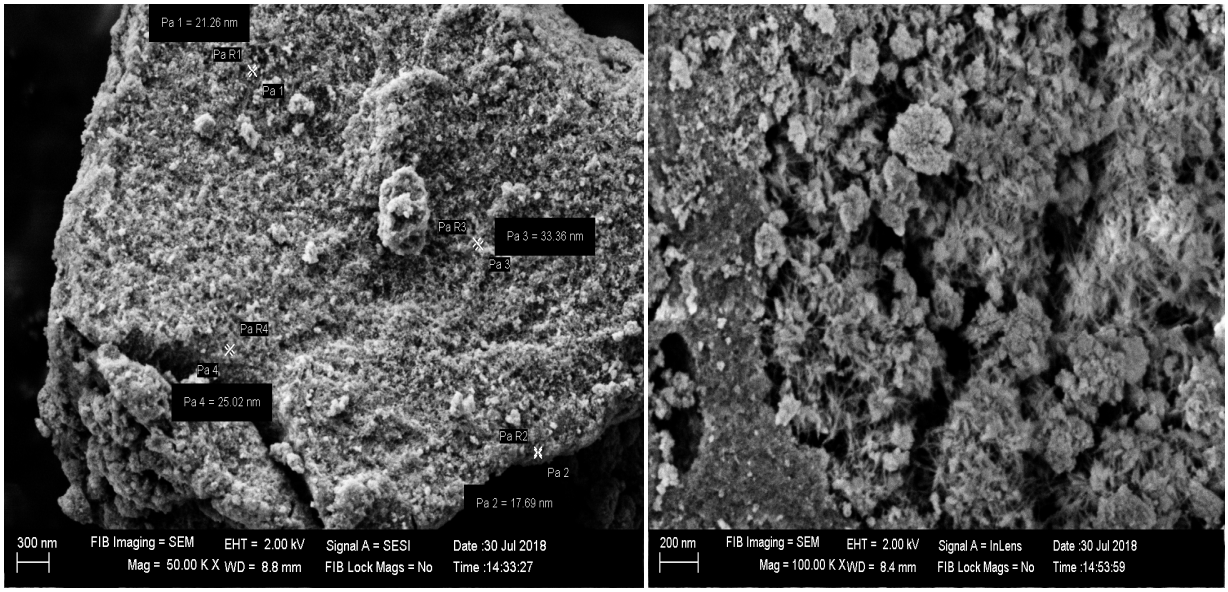

(a) (b)

Figure 11: SEM images of Fe_3O_4 Nps using tween-80 surfactant with different magnifications

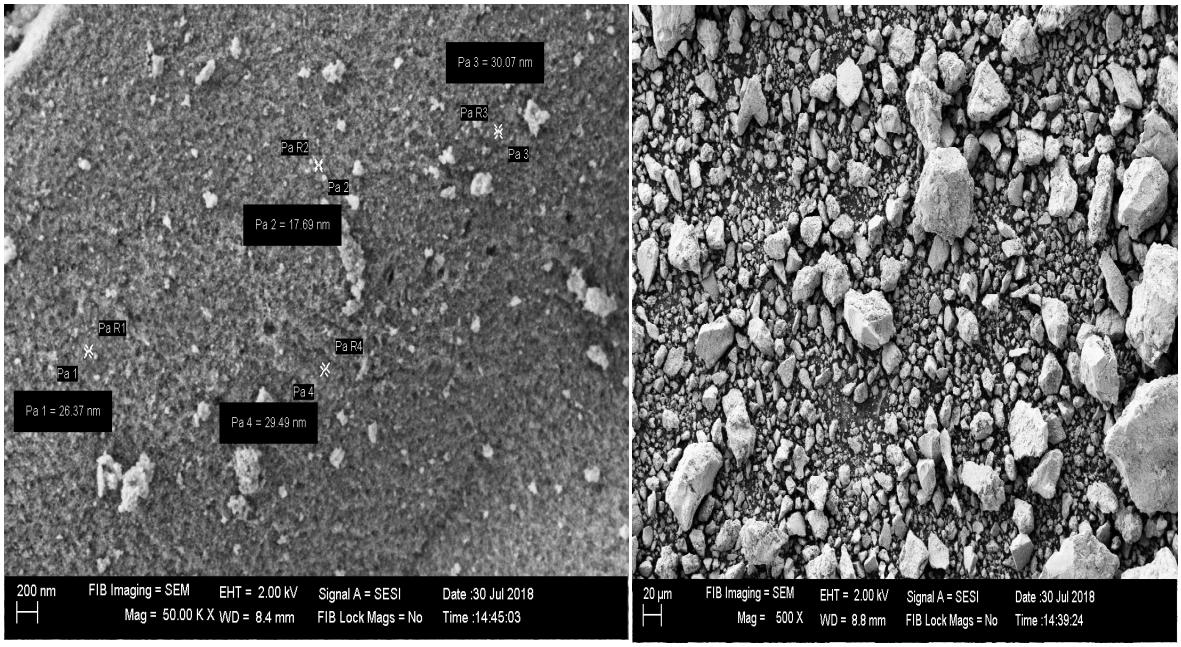

(a) (b)

Figure 12: SEM images of Fe_3O_4 Nps using SDS surfactant with different magnification

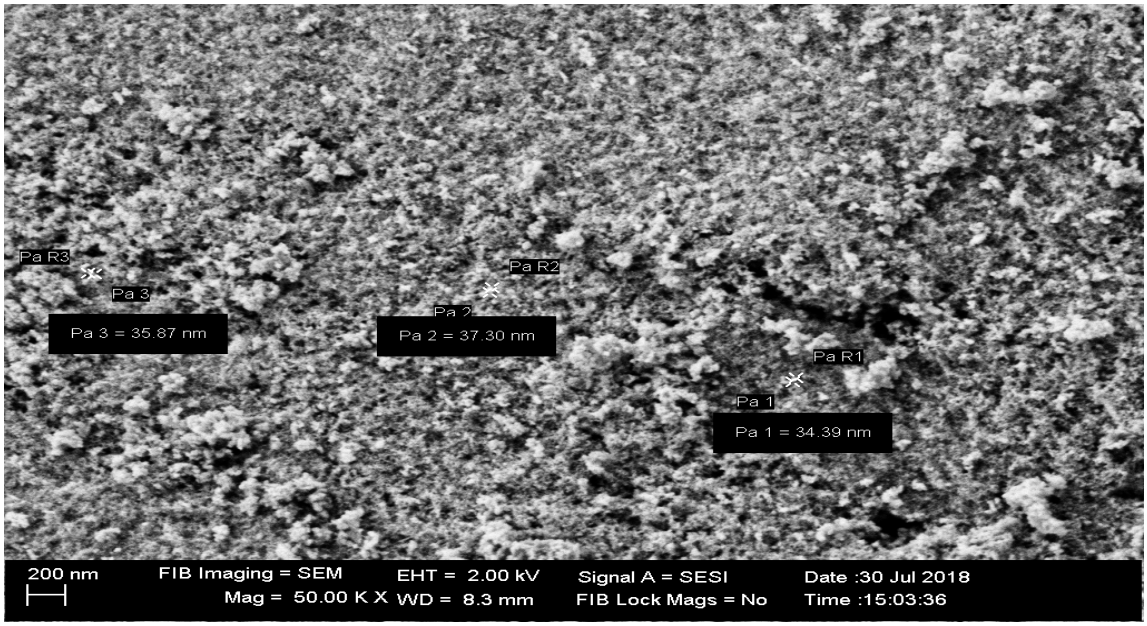

Figure 13: SEM image of Silica coated Fe_3O_4 Nps

4.2. Antimicrobial Study

As indicated in Table 6 the result revealed as the microorganisms are sensitive to the test samples in varying magnitudes. According to the results obtained from Tables 6 the maximum inhibition activity is happened for Ps. aeroginosa bacteria in 15 mg/mL concentrations by Fe_3O_4-30T and Fe_3O_4-30 SDS sample i.e. its zone of inhibition was 19 mm. It is followed by silica coated Fe_3O_4 Nps, Fe_3O_4-50T and Fe_3O_4-30T dilute as their zone of inhibition15, 14 and 14 mm respectively. Others Nps sample showed moderate activity against Ps. aeroginosa. Fe_3O_4-30T, Fe_3O_4-30SDS and silica coated Fe_3O_4 Nps showed good activity against E.coli as their zone of inhibition (ZOI) was 18 mm. It is followed by Fe_3O_4-50T and Fe_3O_4-30T conc. as their zone of inhibition 17 and 15 mm respectively. Fe_3O_4-30 SDS, Fe_3O_4-30Tconc., Fe_3O_4-30T and Fe_3O_4-80 SDS showed good activity against B.subtilus as their zone of inhibition was 14, 14, 13, 13 and 13 mm respectively. Others Nps sample showed least activity against B.subtilus. Silica coated Fe_3O_4 and Fe_3O_4-30T showed good activity against *S.aureus as* their zone of inhibition (ZOI) was 14 and 13mm. Others Nps sample showed least activity against *S.aureus.*

As it is seen clearly from the Table 6 Fe_3O_4-30T and Fe_3O_4-30T from dilute precursor showed better activity against C.ablicans fungi. It is followed by Fe_3O_4-30SDS. Others Nps sample

showed moderate activity against C.ablicans except Fe_3O_4-80T and silica coated Fe_3O_4 nanoparticles which they showed least activity against C.ablicans. Figure 14 demonstrated the similar results which are completely agreed with Tables 6.

The diameter of the inhibition zone shows the antibacterial effect activity of the Fe_3O_4 and silica coated Fe_3O_4 nanoparticles. According to Senthil *et al.* 2012 was reported, it has been seen in this study also that by increasing the concentration of Fe_3O_4 Nps and silica coated Fe_3O_4 Nps in wells the growth inhibition has also been increased (Table 6 and Appendix 1).

Moreover, the diameter of the inhibition zone was completely different according to the different type of bacteria. The size of inhibition zone was different according to the type of bacteria, the size and the concentrations of Fe_3O_4 nanoparticles (Reddy *etal.*, 2007). The results which showed in Tables 6, generally Gram- positive bacteria more resistant to Fe_3O_4 nanoparticles in comparison of Gram-negative bacteria that related to differences in cell wall structure, cell physiology, metabolism or degree of contact.

Table 6: Zone of inhibition (mm) of Fe_3O_4 NPs and silica coated NPs against gram negative and gram positive bacterial strains and c.ablicans fungi

Samples	Zone of inhibition(mm)(Diameter)									
	Gram positive bacteria				Gram negative bacteria				C.ablicans (ATCC9955)	
	Staphylococcus aurous(ATCC 25923)		*Bacillus subtilis (ATCC6633)*		*Escherichia coli(ATCC25922)*		*Pseudomonas aeruginosa*(ATCC7553)			
	C_1 10mg /mL	C_2 15mg/ mL	C_1 10mg/mL	C2 15mg/ mL	C_1 10mg/ mL	C_2 15mg /mL	C_1 10 mg/ mL	C_2 15mg/ mL	C1 1omg/mL	C2 15mg /ML
Fe_3O_4-30T	8	11	10	13	15	18	14	19	11	15
Fe_3O_4-50T	8.	11	8	10	11	15	12	14	9	10
Fe_3O_4-80T	9	11	7	11	6	9	9	11	7	8
Fe_3O_4-30SDS	8	10	9	14	7	11	14	19	12	13
Fe_3O_4-50SDS	9	10	9	12	9	11	8	12	11	12
Fe_3O_4-80SDS	8	10	9	13	13	18	10	12	9	12
Fe_3O_4-30T dil.	8	13	8	13	6	11	9	14	12	14
Fe_3O_4-30T conc.	7	9	7	14	14	17	10	12	11	12
Silica coated Fe_3O_4	10	14	11	12	14	18	7	15	8	10
Gentamacin(+ve)	12		14		14		14		14	
DMSO(-)	No		No		No		No		No	

Many antibacterial studies were made using different nanoparticles. In general, NM act along two major lethal pathways, which are related to each other and in many cases occur simultaneously: disruption of membrane potential and integrity and production of reactive oxygen species (ROS), also known as oxygen-free radicals, the NM acting as nanocatalysts (Beyth, N. et al,2015).

The possible mechanism of action is that the metal nanoparticles are carrying the positive charges and the microbes are having the negative charges which create the electromagnetic attraction between the nanoparticles and the microbes. When the attraction is made, the microbes get oxidized and die instantly (Rezaei-Zarchi, S. et al 2010). Generally, the nanomaterials release ions, which react with the thiol groups (–SH) of the proteins present on the bacterial cell surface which leads to cell lysis.

The central mechanism that caused the antibacterial activity by the particles might be through oxidative stress caused by ROS (Tran, N., et al, 2010). ROS includes radicals like superoxide radicals (O_2^-), hydroxyl radicals (^-OH) and hydrogen peroxide (H_2O_2); and singlet oxygen ($^{-1}O_2$) could be the reason damaging the proteins and DNA in the bacteria. ROS could have been produced by the present metal oxide (Fe_3O_4 Nps) leading to the inhibition of most pathogenic bacteria like S. aureus,*B. subtilis*, *E. coli* and P. aeroginosa .

Figure 14: Antimicrobial activities of different Fe_3O_4 Nps sample and silica coated Fe_3O_4 Nps on four bacteria strain and Candida ablicans fungi

5. CONCLUSION AND RECOMMENDATION

5.1. Conclusions

In this research work pure Fe_3O_4 Nps and silica coated magnetite nanoparticle was synthesized via micro emulsion method using Tween-80 and SDS surfactant. The synthesized magnetite nanoparticles showed relatively small size. Thus, Microemulsion method was found to be an effective method to get controllable size nanoparticles. In the synthesis of Fe_3O_4 Nps by microemulsion method there is a slight size change by varying temperature and precursor concentration. Fourier transforms infrared spectra and X-ray diffraction showed that the Fe_3O_4 NPs were successfully coated by silica. The SEM result showed that the morphology of Fe_3O_4 nanoparticles synthesized using Tween-80 is uniformly distributed with flower like shape. The materials synthesized with Tween-80 showed better antimicrobial properties: on both gram positive and gram negative bacterial strains and Candida ablicans fungi. Silica coated Fe_3O_4 Nps also showed comparable antimicrobial activity with Fe_3O_4 Nps synthesized using Tween-80.

5.2. Recommendation

The following recommendations are made for further study.

- Studies should be carried out on effects of parameter such as amount of water to surfactant ratio, concentration of base, pH for size manipulation of the magnetite and silica coated magnetite Nps.
- This studies reported on application here are conducted on 4 bacteria strain and one fungal strain; future investigation should be carried out on application of waste water treatment, heavy metal removal, electronic device and on additional bacteria and fungi.

6. REFERENCES

Ameer Azam. (**2012**).Antimicrobial activity of metal oxide nanoparticles against Gram-positive and Gram-negative bacterias, a comparative study, **7**, 6003- 6009.

Andrade A. L, Souza D. M. , Pereira M. C., Fabris J. D., Domingues R. Z. (**2009**). Synthesis and characterization of magnetic nanoparticles coated with silica through a sol-gel approach, *Cerâmica,* **55**, 420 - 424.

Anghel A., Grumezescu A., Chirea M. (**2014**). MAPLE fabricated Fe_3O_4*@Cinnamomum verum* antimicrobial surfaces for improved gastrostomy tubes, *Molecules,* **19**(7), 8981- 8994.

Arbain R., Othman, M and Palaniandy, S. (**2011**). Preparation of iron oxide nanoparticles by mechanical milling. *Minerals Engineering*, **24**, 1-9

Arivalagan, K., Ravichandran, S.and Karthikeyan, E., Rangasamy, K. (**2011**). Nanomaterials and its Potential Applications, *International Journal of ChemTech Research,* **3**(2), 534-538.

Asgari, S., Fakhari, Z., Berijani S. (**2014**). Synthesis and Characterization of Fe_3O_4 Magnetic Nanoparticles Coated with Carboxymethyl Chitosan Grafted Sodium Methacrylate, *JNS,* **4**, 55 -63.

Babay, S., Mhiri, T. and Toumi, M. (**2015**).Synthesis, structural and spectroscopic characterizations of maghemite ϒ-Fe_2O_3 prepared by one-step co precipitation route. *J Mol Struct*, 1085, 286-293.

Beyth,N.,Houri-Haddad,Y.,Domb,A., Khan,Wand Hazan,R.(2015). Alternative Antimicrobial Approach: Nano-Antimicrobial Materials, *Evidence-Based Complementary and Alternative Medicine*

Boxall, C., Kelsall, G and Zhang, Z. (**1996**). Photoelectrophoresis of colloidal iron oxides. Part 2-magnetite (Fe_3O_4), *J. Chem. Soc. Faraday Trans*, 92-791.

Cai, Wei; Wan, Jiaqi. (**2007**). Facile synthesis of super paramagnetic magnetite nanoparticles in liquid polyols. *Journal of Colloid and Interface Science*, **305**, 366-370.

Chauhan and Chouhan. (**2012**). International journal of advanced research in pharmaceutical and Biosciences, IJARPB .**2** (3):320-325.

Chen, W.J., Tsai, P.J. and Chen, Y.C. (**2008**). Functional Fe_3O_4/TiO_2 core/shell magnetic nanoparticles as photokillingagents for pathogenic bacteria. Small, **4**, 485–491.

Cornell, R.M and Schwertmann, U. (**2000**). The iron oxides: structure, properties, reactions, occurrences and uses. *Weinheim: Wiley-VCH*

Cristina, P. and Lourdes, C.(**2013**). Performance of the Biocompatible Surfactant Tween 80, for the Formation of Microemulsions Suitable for New Pharmaceutical Processing, **3**, 125-185.

Danielson, B. and Lindman. (**1981**). The definition of a micro emulsion, Colloids and Surfaces, **3**, 391 - 392.

DeAssis DN, Mosqueira VC, Vilela JM, Andrade MS, Cardoso VN. (**2008**). Release profiles and morphological characterization by atomic force microscopy and photon correlation spectroscopy of 99m Technetium-fluconazole nanocapsules. *Int. J. Pharm.*, **349**,152–60.

European Commission (**2011**). "What is a 'nanomaterial'? European Commission breaks new ground with a common definition, European Commission Press release 18 October 2011

Fernandes MTC, Garcia RBR, Leite CAP and Kawachi EY. (**2013**) .The competing effect of ammonia in the synthesis of iron oxide/silica nanoparticles in microemulsion/sol-gel system. Colloids Surf A: *Physicochemical and Engineering Aspects,* **422**, 136-142.

Fernandez, M., Garcia, X.Q., Wangs, C., Belver, J.C., Hanson, J.A., Rodriguez. (**2007**).Anatase TiO_2 nanomaterials: morphological/size dependence of the crystallization and phase behavior phenomena. *J. Phys. Chem.* **111**, 674-682.

Gatoo, A.M., S. Naseem, S., Arfat, Y.M., Dar, M.A., Qasim, K. and Zubair, S. (**2014**). Physicochemical properties of nanomaterials: implication in associated toxic manifestations, *Bio Med Research International* 2014(498420), 8.

Gholami, A.(2016). Lipoamino-acid-coated iron oxide nanoparticle, *Minerva Biotechlogica***, 28**(4),177-86.

Gordon, R.T., Hines J.R., Gordon D.(**1979**). Intracellular hyperthermia. A biophysical approach to cancer treatment via intracellular temperature and biophysical alterations.*MedHypothesis* **,5,** 83-102.

Gubin, S. P., Koksharov, Y. A. , Khomutov, G. B. , Yurkov G. Y. , (**2005**) Magnetic nanoparticles: preparation, structure and propertiesRussian Chemical Reviews **74**, 489-520.

Gupta, A.K., Gupta M. (**2005**). Synthesis and surface engineering of iron oxide nanoparticles

Hu, J., Chen, G. and Lo, I. M. C. (**2005**). Removal and recovery of Cr (VI) from wastewater by maghemite nanoparticles. *Water Research*, **39**(18), 4528 - 36.

Jitendra, N., Tiwari, Rajanish, N., Tiwari, Kwang S., Kim. (**2012**). Progress in Materials Science **57** ,724 - 803.

Jores K, Mehnert W, Drecusler M, Bunyes H, Johan C, MAder K. (**2004**). Investigation on the stricter of solid lipid nanoparticles and oil-loaded solid nanoparticles by photon correlation spectroscopy, field flow fractionasition and transmission electron microscopy. *J Control Release*, **17**, 217-27.

Kim, K., Kim, S., Choa Y. and Kim H.(**2007**). Journal of Magnetite Fe_3O_4 nanoparticles synthesis by wet chemical reduction and their characterization *Ind. Eng. Chem*, **13**, 1137.

Kulkarni AS, Sawadh SP, Palei KP.(**2014**). Synthesis and characterization of superparamagnetic Fe_3O_4@SiO_2 nanoparticles. *J Korean Chem. Soc*, **58**(1), 100-5.

Legodi, M.A. and de Waal, D. (**2007**). The preparation of magnetite, goethite, hematite and maghemite of pigment quality from mill scale iron waste. *Dyes and Pigments*, **74** (1), 161-168.

Lesnikovich, A. I.; Shunkevich, T. MNaumenko, V. N.;Vorobyova, S. A.; Baykov, M. V. (**1990**). Dispersity of magnetite in magnetic liquids and the interaction with a surfactant, *Journal of Magnetism and Magnetic Materials,* **85**(1-3), 14-16.

Lopez-Quintela, M.A. (**2003**). Synthesis of nanomaterials in microemulsions formation mechanism and growth control. Curr. Opin. Coll. Int. Sci. **8**,137-144.

Luechinger .N.A., Grass, R.N., Athanassiou, E.K. and Stark, W.J. (**2010**). *Journal of material Chemistry.5-10*

Machala, L., Tucek, J. and Zboril, R. (**2011**). Polymorphous transformations of nanometric iron (III) oxide: *a review. Chem. Mater* **23**(14), 3255-3272.

Mahmoudi M, Sant S, Wang B, Laurent S, Sen T. (**2011**). Superparamagnetic iron oxide nanoparticles (SPIONs): development surface modification and applications in chemotherapy. *Adv Drug Deliv*, **63**, 24-46.

Mandal, M., Kundu, S., Ghosh, S.K., Panigrahi, S. Sau, T.K.; Yusuf, S.M. and Pal, T. *J.,* (**2005**). *Colloid Interface Sci*.**286**, 187.

Martínez, G., Malumbres, A., Mallada, R., Hueso, J., Irusta, S., Bomatí-Miguel, O and Santamaría, J. (**2012**). Use of a polyol liquid collection medium to obtain ultrasmall magnetic nanoparticles by laser pyrolysis Nanotechnology **23**(425605), 85-92.

Massart, R. (**1981**). Preparation of aqueous magnetic liquids in alkaline and acidic media. *IEEE Trans. Magn.***17(**2**)**, 1247 – 1248.

Moahapatra, M. and Anand, S. (**2010**). Synthesis and applications of nanostructured iron oxides/hydroxides: *Int J Eng Sci Technol* **2** (8), 127-146.

Mohanty, U.S. (**2011**). Electrode position: a versatile and inexpensive tool for the synthesis of nanoparticles, nanorods, nanowires, and nanoclusters of metals, J. *Appl. Electrochem*, **41**, 257-270.

Morel, A. L., Nikitenko, S. I., Gionnet, K. , Wattiaux, A. , J. Lai-Kee-Him, C. Labrugere, B. Chevalier, G. Deleris, C. Petibois, A. Brisson and M. Simonoff. (**2008**).Sonochemical approach to the synthesis of Fe_3O_4@SiO_2core-shell nanoparticles with tunable properties *ACS Nano* **2**(5), 847-856.

Nazari, M., Ghasemi, N., Maddah, H. and Motlagh, M.M. (**2014**). Synthesis and characterization of maghemite nanopowders by chemical precipitation method, *International Journal of Nanostructure Chemistry,* **4**, 44-65

Nitha *et al.*, **(2012**).Antibacterial activity of some selected Indian medicinal plants .*IJPSR* **3**(7), 2038-2042.

Oberdorster, G., Stone, V. and Donaldson, K. (**2007**). Toxicology of nanoparticles: a historical perspective. *Nanotoxicology* **1** (1), 2–25.

Opez-Cuenca, L.S. (**2011**). *High-Yield Synthesis of Zinc Oxide Nanoparticles from Bicontinuous Microemulsions, Journal of Nanomaterials,* **6**, pages doi:10.1155/2011/431382

Oskay, E. (**2003**). Treatment of waste water using magnetite. Dokuz Eylül University Graduate Schooof Natural and Applied Sciences, Turkey.

Perkampus. H.H. (**1992**). UV-VIS spectroscopy and its applications, Springer-Verlag, Berlin, Germany.

Pileni, M. P. (**2003**).The role of soft colloidal templates in controlling the size and shape of inorganic nanocrystals. *Nat. Mater. **2***,145.

Pokropivny, V.V., Skorokhod, V.V. (**2007**).Classification of nanostructures by dimensionality and concept of surface forms engineering in nanomaterial science, *Materials Science and Engineering: C*, ***27(5-8), 990-993.***

Prabhu, Y.T. (**2015**). Synthesis of Fe_3O_4 nanoparticles and its antibacterial application, **5**, 85-92.

Rahmawati, R., Taufiq, A., Suyatman S., Kurniadi, D. (**2018).** Synthesis of Magnetite (Fe_3O_4) Nanoparticles from Iron sands by Co-precipitation-Ultrasonic Irradiation Methods, *J. Mater. Environ. Sci*., **9**(1), 155-160

Rani, S. and Gupta, N. (**2014)**. *International Journal of Materials Science and Engineering*, **2**, 99-106.

Reddy K.M., Kevin F., Jason B., Denise G.W., Cory H. and Alex P. (**2007**). Selective toxicity of zinc oxide nanoparticles to prokaryotic and eukaryotic systems, *J. Appl. Phys. Lett*., **90**(21), 1 3.16.

Rezaei-Zarchi, S., Javed, A., Ghani, M.J., Soufian, S., Firouzabadi, F.B., Moghaddam, A.B. and Mirjalili, S.H. (**2010**). Comparative study of antimicrobial activities of TiO_2 and CdO nanoparticles against the pathogenic strain of Escherichia coli. *Iran J Pathol* **5**(2), 83 – 89.

Salazar-Alvarez G. (**2004**). Synthesis, characterization and application of iron oxide Doctoral Thesis, Stockholm, Sweden.

Santra, S.; Tapec, R.; Theodoropoulou, N.; Dobson, J.; Hebard, A.;Tan, W.(**2001).** Synthesis and characterization of silica -coated iron oxide nanoparticles**,** *Langmuir*, ***17(10)***, 2900-2906.

Saviuc, C., Grumezescu, A.M., Chifiriuc, M.C., Bleotu, C., Stanciu, G., Hristu, R., Mihaiescu, D. and Lazar, V. (**2011**). *In vitro* methods for the study of artificial fungal biofilms. *Biointerface Res Appl Chem*, **1**(1), 31–40.

Senthil, M. and Ramesh, C. (**2012**). Biogenic synthesis of Fe_3O_4 nanoparticles using tridax procumbens leaf extract and its antibacterial activity on pseudomonas aeruginosa. *Dig J Nanomater Biostruct*. **3**, 1655-1660.

Shakeel Ahmed. A. (**2017**). Antibacterial activity of iron oxide nanoparticles synthesized by co-precipitation technology against *Bacilluscereus* and *KlebsiellapneumoniaeTech., Polish Journal of Chemical Technology, **19(4),**110-115.*

Shen, Y.F. (**2009**). Tailoring size andstructural distortion of Fe_3O_4 nanoparticlesfor the purification of contaminated water, *Bioresource Technology*, **100**(18), 4139-4146.

Sibokoza, S. B., Moloto, M. J., Moloto, N., Sibiya P. N. (**2017**).The effect of temperature and precursor concentration onthe synthesis of cobalt sulphide nanoparticles using cobalt diethyl dithiocarbamate complex, *Chalcogenide Letters ,***14**, 69 -78.

Siesler, H.W. and Holland-Moritz, K. (**1980**). Infrared and Raman spectroscopy of polymers, M. Dekker, New York, USA.

Silvia Villa, Paola Riani, Federico Locardi and Fabio Canepa**.** (**2016**). Functionalization of Fe_3O_4 NPs by silanization use of amine (APTES) and thiol (MPTMS) silanes and their physical characterization, *materials,* **9**(10), 826

Singh, R., Smitha, M.S. & Singh, S.P. (**2014**). The role of nanotechnology in combating multi-drug resistant bacteria, *J. Nanosci. Nanotechnol. **14**(7),* 4745-4756.

Soler-Illia, G., Sanchez, C., Lebeau, B. and Patarin, J. (**2002**). Chemical strategies to design textured materials, *Chem. Rev*, **102**, 4093.

Sonmez, M., Andronescu, E., Georgescu, M., Alexandrescu, L. Ficai, L. (**2015**).Synthesis and Applications of Fe_3O_4/SiO_2 Core-Shell Materials, *Current Pharmaceutical Design,**21**,* 000-000.

Srivastava, M., Chaubey, A. and Ojha, A.K. (**2009**). Investigation on size dependent structural and magnetic behavior of nickel ferrite nanoparticles prepared by sol-gel and hydrothermal methods. *Mater Chem Phys **118***(1), 174-180.

Sun, Y., Duan, L., Guo, Z., DuanMu, Y., Ma, M., Xu, L., Zhang, Y. and Gu, N. (**2005**) .An improved way to prepare super paramagnetic magnetite-silica core-shell nanoparticles for possible biological application, *Journal of Magnetism and Magnetic Materials* **285,** 65–70.

Sundeep, H., Hwei-Jang, Y., Jow-Lay H. (**2012**). *Int. J. Nanoscience, **9***(3), 225.

Teja, S.A. and Koh, P.Y. (**2009**). Synthesis, properties, and applications of magnetic iron oxide nanoparticles, *Prog Cryst Growth Charact Mater*, ***55***(1-2), 22-45.

Tran, N., Mir, A., Mallik, D., Sinha, A., Nayar, S. and Webster, T.J. (**2010**). Bactericidal effect of iron oxide nanoparticles on Staphylococcus aureus, *Int J Nanomed,* **5**(1), 27-283.

Wang, X.,Zhuang, J. Peng, Q and Li, Y.D. (**2005**).A general strategy for nanocrystal synthesis. *Journal of Nature*, **437**, 121-124.

WHO. (**2011**). *Guidelines for Drinking Water Quality-Fourth Edition*, World Health Organization, Geneva.

Willard, M.A., Kurihara, L.K., Carpenter, E.E., Calvin, S. and Harris, V.G. (**2004**).Chemically Prepared Magnetic Nanoparticles, Int*. Mater. Rev, **36***, 125-170.

Wongwailikhit, K and Horwongsakul, S. (**2011**). The preparation of iron (III) oxide nanoparticles using W/O microemulsion, *Materials Letters,* **65**, 2820-2822.

Wu, W., Quanguo He and Changzhong Jiang. (**2008**). Magnetic Iron Oxide Nanoparticles: Synthesis and Surface Functionalization Strategies, *Nanoscale Res Lett* **3**, 397-415.

Wu, W., Xiao, X. H., Zhang, S. F., Zhou, J. A., Fan, L. X., Ren, F. and Jiang, C. Z. (**2010**). Large-scale and controlled synthesis of iron oxide magnetic short nanotubes: shape evolution, growth mechanism, and magnetic properties, *J. Phys. Chem. C* , **22**, 155-160.

Xu, H., Wang, X. and Zhang, L. (**2008**). Selective preparation of nanorods and micro-octahedrons of Fe_2O_3 and their catalytic performances for thermal decomposition of ammonium perchlorate, *Powder Technol **185***(2), 176-180.

Xuan Nui Pham et. al. (**2016**). Synthesis and characterization of chitosancoatedmagnetite nanoparticles and theirapplication in curcumin drug delivery, *Adv. Nat. Sci: Nanosci. Nanotechnol.* 7 045010.

Yunusa, S., Ahmed, A.S., Bawa, S.G., Iyun, J.F. and Dauda M. (**2016***).* Preparation of High Grade Silica from Rice Husk for Zeolite Synthesis, *Nigerian Journal of Basic and Applied Science . **24**(1),41-45*.

Zboril, R., Mashlan, M. and Petridis, D. (**2002**). Iron (III) oxides from thermal processes-synthesis, structural and magnetic properties, Mossbauer spectroscopy characterization, and applications, *Chem Mater **14**(*3), 969-982.

Zhang, C., Wangler, B., Morgenstern, B., Zentgraf, H., Eisenhut, M., Untenecker, H., Kruger, R., Huss, R., Seliger, C., Semmler, W. and Kiessling, F**. (2007).**Silica- and alkoxysilane-coated ultrasmall superparamagnetic iron oxide particles: a promising tool to label cells for magnetic resonance imaging**,** *Langmuir*, ***23***(3), 1427-34.

7. APPENDIXES

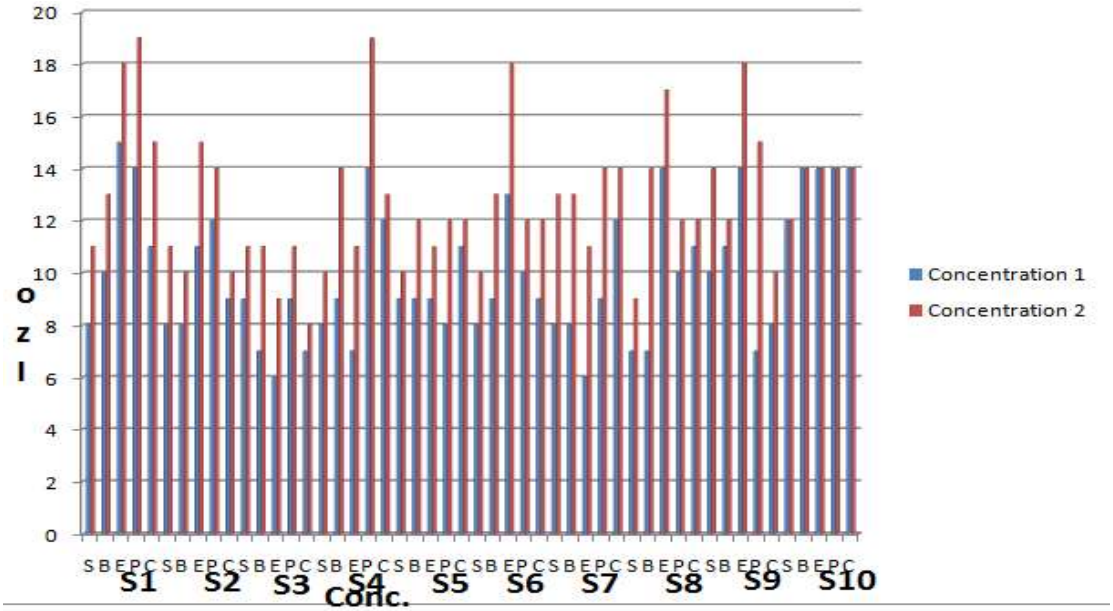

Appendix 1: Inhibition zone verses concentration Nps graph against the microbial strains

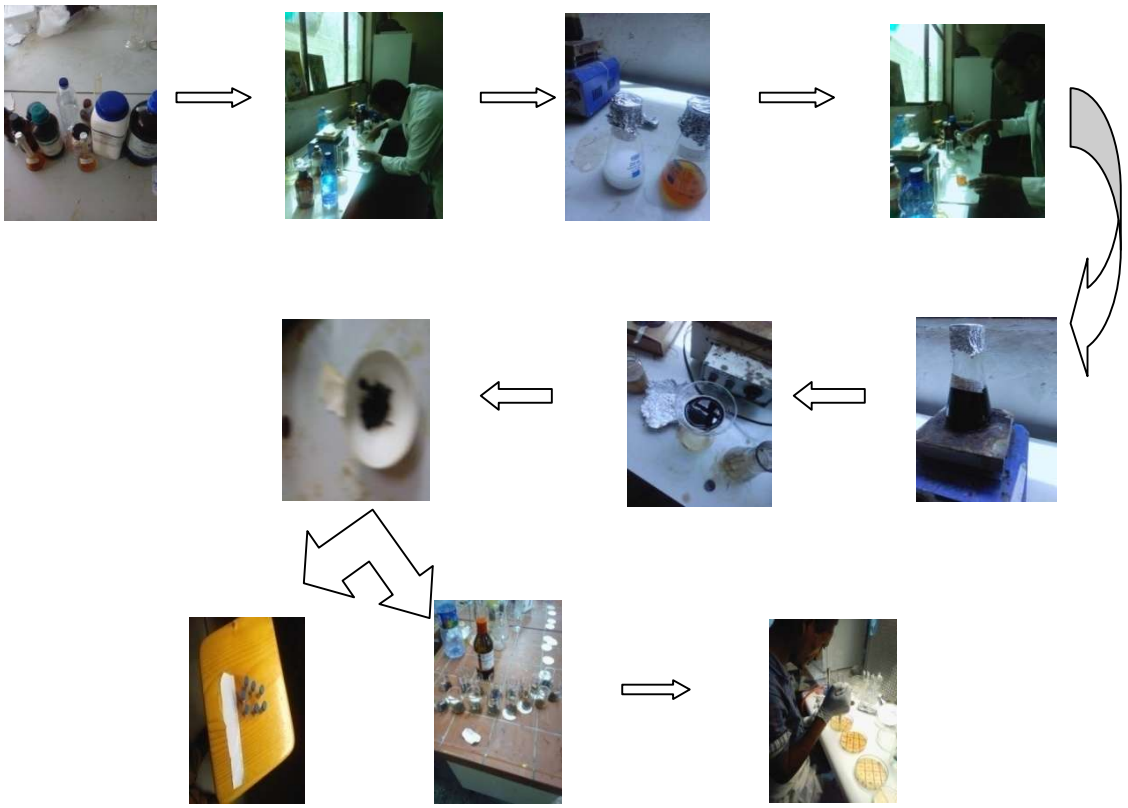

Appendix 2: Pictorial representation of the synthesis process for Fe_3O_4 Nps